

NATL INST. OF STAND & TECH R.I.C.  
A11104 123923

NIST  
PUBLICATIONS

**NISTIR 5251**

---

# Zone Fire Modeling With Natural Building Flows and a Zero Order Shaft Model

---

John H. Klotz  
Glenn P. Forney

Building and Fire Research Laboratory  
Gaithersburg, Maryland 20899

~~QC~~

100

.U56

#5251

1993

**NIST**

United States Department of Commerce  
Technology Administration  
National Institute of Standards and Technology



# Zone Fire Modeling With Natural Building Flows and a Zero Order Shaft Model

---

John H. Klotz  
Glenn P. Forney

September 1993  
Building and Fire Research Laboratory  
National Institute of Standards and Technology  
Gaithersburg, MD 20899



**U.S. Department of Commerce**  
Ronald H. Brown, *Secretary*  
**Technology Administration**  
Mary L. Good, *Under Secretary for Technology*  
National Institute of Standards and Technology  
Arati Prabhakar, *Director*



## Table of Contents

List of Tables . . . . .	iv
List of Figures . . . . .	v
Abstract . . . . .	1
Nomenclature . . . . .	1
1. Introduction . . . . .	2
2. Stack Effect . . . . .	3
3. Zone Fire Models . . . . .	5
4. Applicability of Two Zone Model for Shafts . . . . .	6
5. Zone Model Modifications . . . . .	8
5.1 Zero Order Shaft Model . . . . .	8
5.2 HVAC Heating . . . . .	9
5.3 Upper Layer Initiation . . . . .	9
6. Computer Simulations . . . . .	10
6.1 Effect of HVAC Heating Without a Fire . . . . .	10
6.2 First Floor Fire and Normal Stack Effect . . . . .	30
6.3 First Floor Fire and Reverse Stack Effect . . . . .	32
6.4 3rd Floor Fire and Reverse Stack Effect . . . . .	33
6.5 Layer Initiation Temperature . . . . .	33
7. Future Effort . . . . .	34
8. Conclusions . . . . .	34
9. References . . . . .	35



**List of Tables**

Table 1. Building flow areas for runs with modified zone model . . . . . 11

Table 2. Conditions of runs with modified zone model . . . . . 12

Table 3. Steady fire temperatures and CO concentrations . . . . . 31





## List of Figures

Figure 1.	Air movement due to normal and reverse stack effect . . . . .	3
Figure 2.	Shafts connected to the outside by (a) one continuous opening, and (b) an opening at the top and another at the bottom . . . . .	5
Figure 3.	Fire plume and idealized model of axisymmetric, point source plume . . . . .	6
Figure 4.	Zone model idealization of a compartment fire . . . . .	7
Figure 5.	Zone model idealization of a compartment fire . . . . .	7
Figure 6.	Wall plume . . . . .	8
Figure 7.	Example eight story building for zone model calculations . . . . .	10
Figure 8.	Temperatures from runs 1 and 2 . . . . .	13
Figure 9.	Interface heights on fire floor (floor 1) for runs 3, 4 and 5 . . . . .	13
Figure 10.	Interface heights on floor 8 for runs 3, 4 and 5 . . . . .	14
Figure 11.	Interface height in shaft for runs 3, 4 and 5 . . . . .	14
Figure 12.	Temperature on fire floor (floor 1) for runs 3, 4 and 5 . . . . .	15
Figure 13.	Temperature on floor 8 for runs 3, 4 and 5 . . . . .	15
Figure 14.	Temperature in shaft for runs 3, 4 and 5 . . . . .	16
Figure 15.	CO concentration on fire floor (floor 1) for runs 3, 4 and 5 . . . . .	16
Figure 16.	CO concentration on floor 8 for runs 3, 4 and 5 . . . . .	17
Figure 17.	CO concentration in shaft for runs 3, 4 and 5 . . . . .	17
Figure 18.	Temperatures from runs 6 and 7 . . . . .	18
Figure 19.	Interface heights on floor 8 for runs 10, 11 and 12 . . . . .	18
Figure 20.	Interface height in shaft for runs 10, 11 and 12 . . . . .	19
Figure 21.	Temperature on floor 8 for runs 10, 11 and 12 . . . . .	19
Figure 22.	Temperature in shaft for runs 10, 11 and 12 . . . . .	20
Figure 23.	CO concentration on floor 8 for runs 10, 11 and 12 . . . . .	20
Figure 24.	CO concentration in shaft for runs 10, 11 and 12 . . . . .	21
Figure 25.	Interface heights on floor 8 for runs 13, 14 and 15 . . . . .	21
Figure 26.	Interface height in shaft for runs 13, 14 and 15 . . . . .	22
Figure 27.	Temperature on floor 8 for runs 13, 14 and 15 . . . . .	22
Figure 28.	Temperature in shaft for runs 13, 14 and 15 . . . . .	23
Figure 29.	CO concentration on floor 8 for runs 13, 14 and 15 . . . . .	23
Figure 30.	CO concentration in shaft for runs 13, 14 and 15 . . . . .	24
Figure 31.	Interface Heights for runs 6 and 16 . . . . .	24
Figure 32.	Temperatures for runs 6 and 16 . . . . .	25
Figure 33.	Interface heights on floor 8 for runs 12 and 17 . . . . .	25
Figure 34.	Interface height in shaft for runs 12 and 17 . . . . .	26
Figure 35.	Temperature on floor 8 for runs 12 and 17 . . . . .	26
Figure 36.	Temperature in shaft for runs 12 and 17 . . . . .	27
Figure 37.	CO concentration in shaft for runs 12 and 17 . . . . .	27
Figure 38.	Interface heights on floor 8 for runs 15 and 18 . . . . .	28
Figure 39.	Temperature on floor 8 for runs 15 and 18 . . . . .	28

## List of Figures Continued

Figure 40. Temperature in shaft for runs 15 and 18 . . . . .	29
Figure 41. CO concentration on floor 8 for runs 15 and 18 . . . . .	29
Figure 42. CO concentration in shaft for runs 15 and 18 . . . . .	30

# Zone Fire Modeling with Natural Building Flows and a Zero Order Shaft Model

John H. Klotz  
Glenn P. Forney

## Abstract

This paper addresses applications of zone fire models to simulate smoke flow in multistory buildings. Natural flows in buildings are discussed. A zero order model for shaft smoke flow was developed which treated the shaft as one perfectly mixed zone. A two zone fire model was modified to simulate natural flows and the zero order shaft smoke flow. The extent to which the one zone model and the two zone model are appropriate to simulate smoke flow in shafts is discussed. The modifications for the natural building flow included development of new initial conditions and of the capability to simulate the gross effects of a heating and air conditioning system. Eighteen example zone model simulations were made to develop insight into the program modifications.

## Nomenclature

$A_a$	= area above neutral plane
$A_b$	= area below neutral plane
$C_p$	= constant pressure specific heat
$D$	= plume diameter at $z$
$H$	= height of shaft
$H_n$	= distance from the bottom of the shaft to the neutral plane
$m_{ij}$	= mass flow rate from room (or other space) $j$ to room $i$
$T_b$	= absolute temperature of gas outside the fire space
$T_f$	= absolute temperature of gas in the fire compartment
$T_o$	= absolute temperature of outside air
$T_j$	= absolute temperature of mass flow rate $m_{ij}$
$T_s$	= absolute temperature of air in shaft
$T_{l,i}$	= absolute temperature of lower layer of room $i$
$T_{u,i}$	= absolute temperature of upper layer of room $i$
$P_{atm}$	= absolute atmospheric pressure
$R$	= gas constant of air
$g$	= acceleration of gravity
$Q_{HVAC,i}$	= rate of heat release from the HVAC system into space $i$
$z$	= height above the neutral plane, or height above virtual origin of plume
$\alpha$	= aspect ratio (shaft height to shaft width)

# 1. Introduction

In building fires, smoke often migrates to building locations remote from the fire space, threatening life and damaging property. Stairwells and elevator shafts frequently become smoke-logged, thereby blocking evacuation and inhibiting rescue and fire fighting. The MGM Grand Hotel fire (Best and Demers 1982) is an example of such a smoke problem. The fire was limited to the first floor, but smoke spread throughout the building. Some occupants on upper floors were exposed to smoke for hours before rescue. The death toll was 85, and the majority of the deaths were on floors far above the fire. The MGM Grand is not unique in this respect as is illustrated by the fires at the Roosevelt Hotel (Juillerant 1964) and Johnson City Retirement Center (Steckler, Quintiere and Klote 1990). All these fires were located on the first floor, but the majority of deaths were on upper floors. These fires illustrate the importance of smoke flow through shafts.

This paper is part of NIST's Large Scale Smoke Movement Project. This paper addresses applications of zone fire models to simulate smoke flow in multistory buildings. This paper presents a discussion of the natural flows and a zero order model for modeling smoke flow in shafts. A zone model was modified to simulate natural flows and the zero order shaft smoke flow. The modifications for the natural building flow included development of new initial conditions and of the capability to simulate the heating and cooling of a heating, ventilation and air conditioning (HVAC) system. Eighteen example zone model simulations were made to develop insight into the program modifications. The intent of this study was to develop an understanding of some of requirements for applying zone models to smoke movement in multistory buildings. Additionally, it is anticipated that this paper may be of benefit to those interested in modeling smoke movement in large buildings.

Tanaka (1983) has simulated smoke flow in a multistory building, but his analyses do not include the zone model modifications discussed above. An alternate approach to zone modeling for large scale smoke flow is network modeling, and Said (1988) discusses the features and capabilities of several network smoke flow models. Network models do not include either thermal expansion or the development of hot upper layers of fire gases. The impact of these limitations has yet to be evaluated for network models, and this topic is beyond the scope of this paper.

Evers and Waterhouse (1978) developed a zero order shaft model for their network smoke flow model. The zero order model used in this paper treats the shaft as one perfectly mixed zone, and to some extent this is similar to the approach of Evers and Waterhouse, which is discussed later. Cannon and Zukoski (1976) studied the instability and turbulent mixing of hot lower layer in a shaft only open at the bottom. Marshall (1985 and 1986) conducted experiments of smoke flow in open shafts and stair shafts not subject to natural building flows. Further research is needed to develop a general shaft smoke flow model for tall shafts subject to natural building flows.

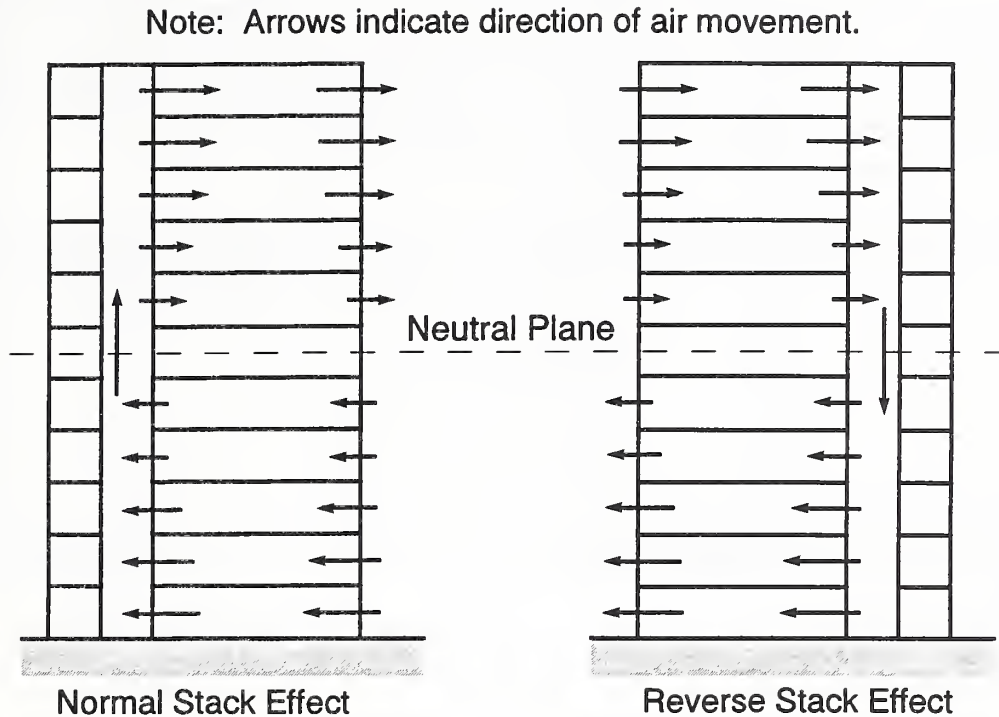


Figure 1. Air movement due to normal and reverse stack effect

## 2. Stack Effect

Stack effect is a major driving force<sup>1</sup> of smoke movement in buildings, and discussion of natural building flows in this paper are limited to those caused by stack effect. However, all of the driving forces of smoke movement result in flows into or out of shafts at each floor. Attention is given to stack effect, because the flow produced by stack effect are easily analyzed. Further, the following analysis can be used to verify a zone model's treatment of flows and pressures due to stack effect. The information in this section is based on that of McGuire and Tamura (1975), and Klote and Milke (1992).

<sup>1</sup>Other driving forces of smoke movement include buoyancy of combustion gases, expansion of combustion gases, wind effect, fan powered ventilation systems, and elevator piston effect. HVAC effects in these simulations consisted of the addition or subtraction of heat from spaces and not mass transfer to or from spaces.



Frequently when it is cold outside, there is an upward movement of air within building shafts, such as stairwells, elevator shafts, dumbwaiters shafts, mechanical shafts, and mail chutes. Air in the building has a buoyant force because it is warmer and therefore less dense than outside air. The buoyant force causes air to rise within building shafts. This phenomenon is called by various names such as stack effect, stack action, and chimney effect. These names come from the comparison with the upward flow of gases in a smoke stack or chimney. However, a downward flow of air can occur in air conditioned buildings when it is hot outside. For this paper, the upward flow will be called normal stack effect, and the downward flow will be called reverse stack effect as illustrated in figure 1.

Most building shafts have relatively large cross sectional areas, and for most flows typical of those induced by stack effect the friction losses are negligible in comparison with pressure differences due to buoyancy. Pressure difference,  $\Delta P$ , due to fluid static forces between a shaft and the outside are

$$\Delta P = \frac{g P_{atm}}{R} \left( \frac{1}{T_o} - \frac{1}{T_s} \right) z \quad (1)$$

where

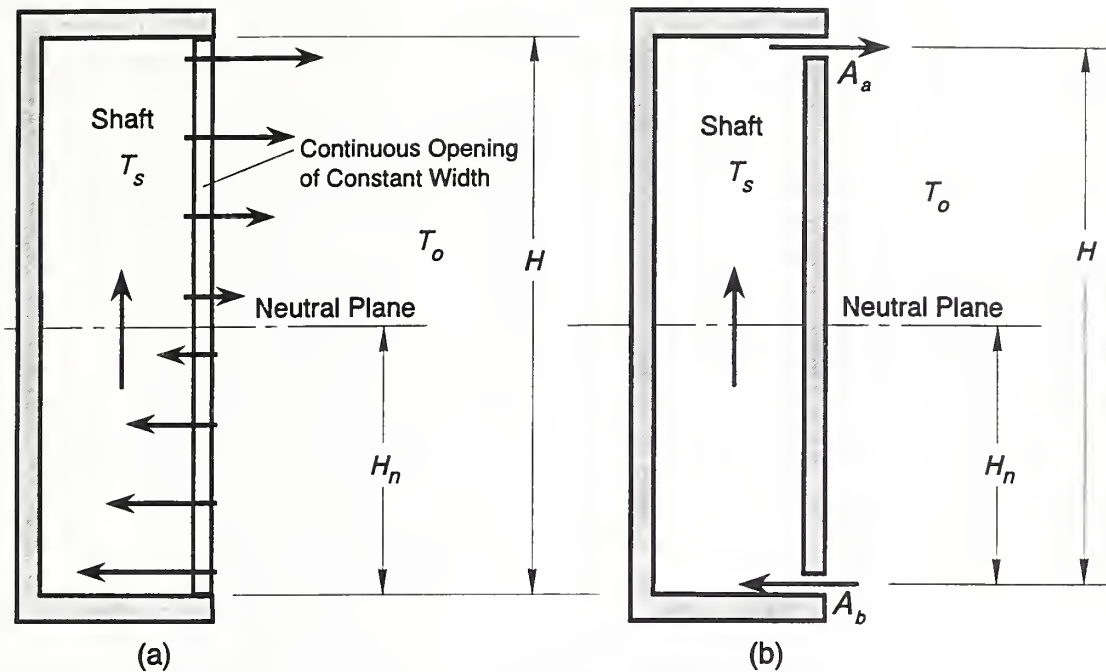
- $T_o$  = absolute temperature of outside air,
- $T_s$  = absolute temperature of air inside the shaft,
- $P_{atm}$  = absolute atmospheric pressure,
- $R$  = gas constant of air,
- $g$  = acceleration of gravity, and
- $z$  = height above the neutral plane.

This equation was developed for a shaft connected to the outside with constant outside temperature and constant inside temperature. The neutral plane is a horizontal plane located at  $z = 0$  where the pressure inside equals that outside as stated above. If the location of the neutral plane is known, equation (1) can be used to determine the pressure difference from the inside to the outside regardless of variations in building leakage or the presence of other shafts.

Unless otherwise stated, the only connections that will be considered in this paper are those between the shaft and the outside. However, the concept of effective flow areas (Klote and Milke 1992) can be used to extend the following analysis to include connections to the building as well. For a shaft connected to the outside by a number of openings, the location of the neutral plane can be found by simultaneously solving the following set of algebraic equations for conservation of mass for the shaft, mass flows through connections, hydrostatic pressure inside the shaft, and hydrostatic pressure outside the shaft. This general solution for the location of the neutral plane for a shaft connected to the outside by any number of openings is presented by Klote (1991), including a computer program for this application.

When the connections between the shaft and the outside are simple, straight-forward equations can be developed. For normal stack effect ( $T_o < T_s$ ), the location of the neutral plane of a shaft that has only one opening of constant width is

$$\frac{H_n}{H} = \frac{1}{1 + (T_s/T_o)^{1/3}} \quad (2)$$



Note: Flow directions shown for normal stack effect.

Figure 2. Shafts connected to the outside by (a) one continuous opening, and (b) an opening at the top and another at the bottom

The opening for the above equations extends the entire height of the shaft as illustrated in figure 2a. Thus the height of the shaft,  $H$ , equals the height of the opening. For a shaft that extends below or above the opening,  $H$  should be taken as the height of the opening.  $H_n$  is the height from the bottom of the opening to the neutral plane. From equation (2), the relative height ( $H_n/H$ ) of the neutral plane is 0.488, for an inside temperature of  $21^\circ\text{C}$  ( $70^\circ\text{F}$ ) and an outside temperature of  $-17^\circ\text{C}$  ( $1^\circ\text{F}$ ). This location is slightly less than the generally accepted approximation of mid-height of the opening. Klotz (1991) presents other equations for the location of neutral planes for reverse stack effect and another connection arrangement.

These steady flow stack effect relations can be used to gain insight into stack effect and to solve practical flow problems. For applications of this paper, these relations were used as an independent check of a zone model's treatment of natural building flows due to buoyant forces.

### 3. Zone Fire Models

There are many different zone fire models including ASET (Cooper 1985), the BRI Model (Tanaka 1983), CCFM (Cooper and Forney 1990), CFAST (Peacock et al. 1993), and the Harvard Code (Mitler and Emmons 1981). While each of these models has unique features, they all share the same basic two zone model concept. This section is an overview of the features that are common to most zone fire

models. For more general information about zone models readers are referred to Bukowski (1991), Quintiere (1989), Mitler and Rockett (1986), Mitler (1985) and Jones (1983).

In a room fire, hot gases rise above the fire forming a plume. As the plume rises, it entrains air from the room so that the diameter and mass flow rate of the plume increase with elevation (figure 3). Accordingly, the plume temperature decreases with elevation. The fire gases from the plume flow up to the ceiling and form a hot layer under it. The hot gases can flow through openings in walls to other spaces, and such flow is referred to as doorjets. The doorjet is similar to a plume in that air is entrained and the mass flow rate and cross-sectional area of the jet increase with elevation, and the jet temperature decreases with elevation. Generally zone models use the same calculation for entrainment for plumes and doorjets, but CFAST modifies entrainment in doorjets to account for the rectangular cross-section of the doorjet. Figure 4 is a sketch of a room fire.

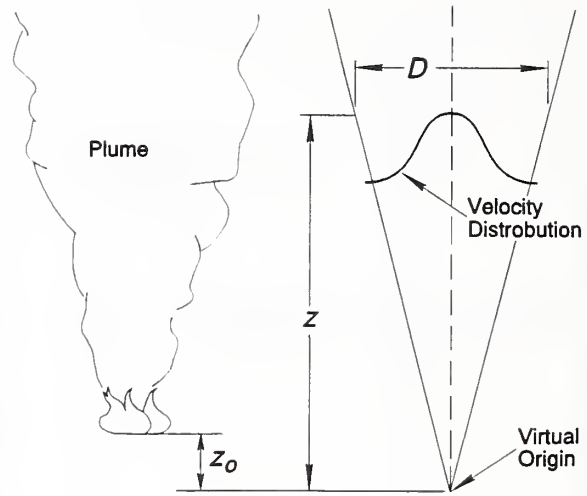


Figure 3. Fire plume and idealized model of axisymmetric, point source plume

The concept of zone modeling is an idealization of the room fire conditions (figure 5). For this idealization the temperature,  $T_{u,i}$ , of the hot upper layer of each room,  $i$ , is uniform, and the temperature,  $T_{l,i}$ , of the lower layer of this room is also uniform. The height of the discontinuity between these layers is the same everywhere. The dynamic effects on pressure are considered negligible, so that the pressures are treated as hydrostatic. Other properties are considered uniform for each layer. Algebraic equations are used to calculate the mass flows due to plumes and doorjets. However, zone models do not simulate the plume or doorjet details (volume, diameter, temperature distribution, velocity distribution, mass flow rate, etc.). Plumes and doorjets are considered to transfer mass instantaneously from a fire or an opening to the upper layer in the appropriate room. This approach to plumes and doorjets is applicable to many room fire situations, but it will be shown later that it is inappropriate for tall shafts.

Zone models estimate heat transfer by methods ranging from a simple allowance as a fraction of the heat released by the fire to complicated simulation including the effects of conduction, convection and radiation. Zone models have proven utility for fire protection applications including hazard analysis (Peacock et al. 1991; Bukowski et al. 1991).

## 4. Applicability of Two Zone Model for Shafts

Smoke can enter a shaft as a doorjet or a plume can be generated due to a fire in the shaft. Because doorjets are very similar to plumes, most of the following discussion concerns plumes. However, the



general ideas apply to doorjets as well. As the plume rises, it widens. The diameter of an axisymmetric plume is approximately half the height above the origin as shown in figure 3 ( $D = 0.5z$ , where  $D$  is diameter, and  $z$  is height above origin). Marshall (1986) showed that a doorjet in a shaft is approximated by half of an axisymmetric plume which is referred to as a wall plume (figure 6). The cross section of a wall plume is a semi-circle, and its mass flow is about half that of an axisymmetric plume. For further information about plumes readers are referred to Klote and Milke (1992).

Where a plume contacts a wall, air is not entrained. However, plume equations currently used in two zone models do not account for this reduced entrainment. For a short shaft with an aspect ratio,  $\alpha$ , less than two ( $\alpha < 2$ , where  $\alpha$  is the ratio of shaft height to shaft width), the probability of plume contact with the walls is low. Thus, a two zone shaft model is applicable for short shafts. Shafts with much greater aspect ratios ( $\alpha \gg 2$ ) are referred to as tall shafts, and smoke flow in this shafts is another matter as discussed below.

The observed smoke flow during full scale experiments at the Plaza Hotel (Klote 1990) is an example of the difference in smoke flow in shafts and in rooms. This project consisted of sprinklered and unsprinklered fires with and without smoke control. The unsprinklered fires without smoke control are of interest in the context of this paper, and stairwell smoke flow was recorded by video cameras on the second floor (fire floor), fourth floor and seventh floor (top of stair). During these fires, a doorjet of smoke flowed into the stairs through gaps around the second floor door. Smoke from this doorjet formed a thin layer (about 0.10 m) under the second floor ceiling in the stairwell and then flowed up into the space between the upward and downward staircases. At about three minutes after ignition, smoke completely fills the field of vision of the fourth floor video camera. This may have been the result of a plug of well mixed smoke reaching the fourth floor. At about eight minutes after ignition, smoke reached the seventh floor. This smoke flow was for weak stack effect conditions, and it is anticipated that stronger stack effect would have speeded up the flow. Reverse stack effect could have a significant impact on

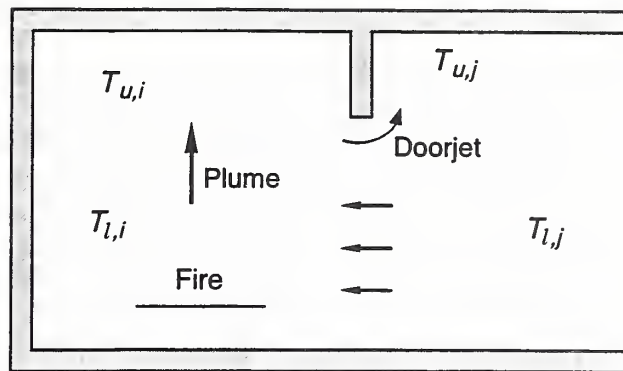


Figure 4. Zone model idealization of a compartment fire

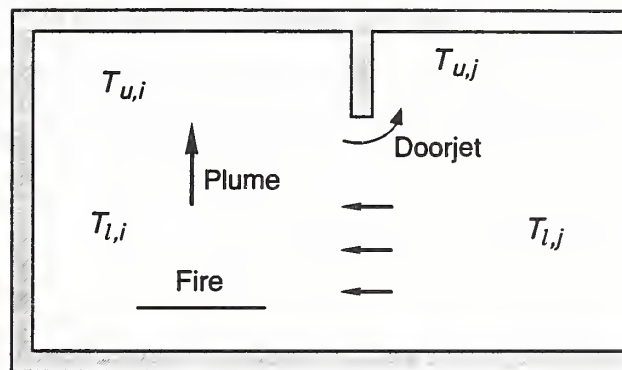


Figure 5. Zone model idealization of a compartment fire

smoke flow, possibly resulting in downward smoke flow. For the Plaza fires, wind effect was not significant, but wind effects could also have a significant impact.

If smoke enters the bottom of a tall shaft, the plume will contact the walls. Accordingly, the mass flow rate of smoke will be significantly overestimated. Currently, two zone models do not consider convective heat transfer from the plume to the shaft walls, so the upper layer temperature would be overestimated. Because plume equations consider mass flow to the upper layer as instantaneous, the flow time to the upper layer is underestimated. However, incorporation of reduced entrainment, convective heat transfer and a time lag in a two zone model would not result in a model that is physically consistent with the mechanisms of shaft smoke flow. Thus there would be no reason to expect such an enhanced two zone model could realistically simulate shaft smoke condition under a wide range of naturally occurring driving forces (normal stack effect, reverse stack effect, wind, etc.). Further research is needed to understand the relevant mechanisms so that a shaft smoke flow model can be developed which can be integrated into two zone models and simulate smoke flow under the wide range of driving forces that occur in buildings. Such a shaft model would be consistent with the mechanisms of shaft smoke flow as the two zone model is consistent with the mechanisms of room smoke flow.

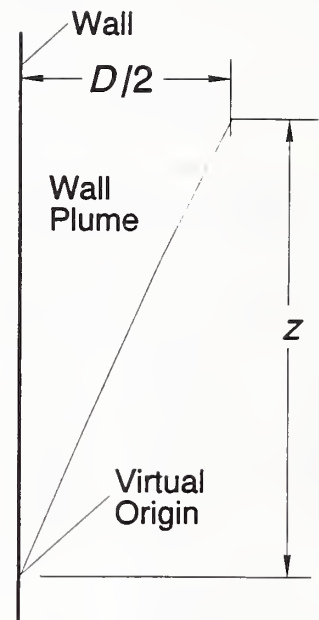


Figure 6. Wall plume

## 5. Zone Model Modifications

In order to evaluate the effects of natural building flows and one zone shaft flows, the CCFM zone model was modified. This model was chosen because its simple structure and capabilities made modification straight-forward. The computer programming involved with these modifications was done in a quick manner, appropriate for evaluation of the modifications but not for public distribution. The treatment of stack effect in the modified zone model was verified by comparison of steady flows and pressures with the stack effect equations above.

### 5.1 Zero Order Shaft Model

The approach used for the zero order shaft model was to consider the shaft as one perfectly mixed zone. This approach was chosen for two reasons. First there often is considerable mixing in shaft flow, so this model should be realistic in some situations. Second the zone fire model could be easily modified to simulate single zone compartments. The shaft model of Evers and Waterhouse (1978) differed in that they treated each floor of a shaft as a separate perfectly mixed zone. The network approach of the Evers and Waterhouse model may have facilitated their approach. Both approaches described above have the limitation that they can not simulate bidirectional flow. Such flow can occur when smoke flows up a shaft during reverse stack effect.

## 5.2 HVAC Heating

Typically, at the start of a zone model simulation, the temperatures are considered constant and mass flows are considered zero. However, the initial condition of zero mass flow is not consistent with building stack effect or other natural building flows. Further, many buildings have HVAC systems that result in constant inside temperatures despite infiltration of outside air.

The model was modified for HVAC heating and the initial conditions of steady mass flows due to stack effect. The steady flows are used to calculate the HVAC heating needed to maintain constant flows and temperatures in the absence of fire. The HVAC heating rate of a room is the sum of the enthalpy flow out of the room less the sum of the enthalpy flow into the room. For constant specific heat, the HVAC heating for room  $i$  is

$$Q_{HVAC,i} = C_p \left[ \sum_j^n (m_{ji} T_{l,i})_{out} - \sum_j^n (m_{ij} T_j)_{in} \right] \quad (3)$$

where

$C_p$  = constant pressure specific heat,

$m_{ij}$  = mass flow rate from room (or other space)  $j$  to room  $i$ ,

$m_{ji}$  = mass flow rate from room  $i$  to room (or other space)  $j$ ,

$T_j$  = absolute temperature of mass flow rate  $m_{ij}$ , and

$T_{l,i}$  = absolute temperature of lower layer of room  $i$ .

The temperature  $T_j$  is either  $T_o$  if space  $j$  is the outside or  $T_{l,j}$  if  $j$  is a room.

## 5.3 Upper Layer Initiation

Often zone models initiate an upper layer if gases from the plume are above a predetermined temperature. This *initiation temperature* is the lower layer temperature plus an *initiation temperature difference*. The default for the zone model of this report was an initiation temperature difference of 1°C (1.8°F). If the building temperature were 21°C (70°F), a plume temperature of 22°C (72°F) or higher results in the formation of an upper layer. Also, gases flowing into a room will initiate an upper layer, provided the gas is above the initiation temperature. These gases may be from another room in the building or from the outside.

In the summer, warm air flowing through building cracks can form an upper layer in the absence of hot fire gases. Such a *phantom* upper layer might only be a few degrees warmer than the lower layer. Delays in fire gases reaching a room can be due to a slow starting fire or a change in an opening during a fire. If fire gases could reach the room after a large phantom layer has formed, and a current two zone model would add these fire gases to the existing upper layer. However, if the fire gases are much hotter than the upper layer, it is expected that they would really form their own hot layer under the ceiling. Thus the formation of a phantom upper layer could result in a simulation with an overestimated upper layer depth and an underestimated upper layer temperature.

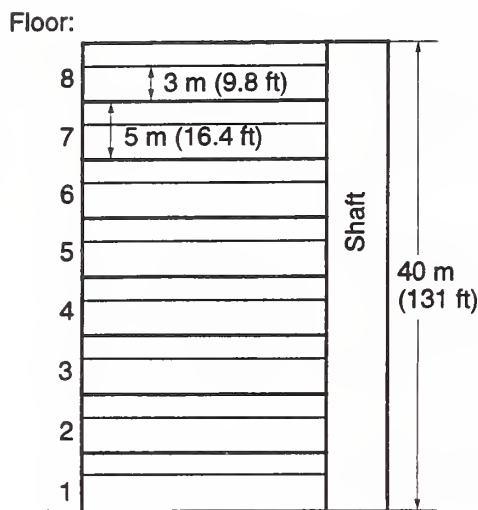


Figure 7. Example eight story building for zone model calculations

The initiation temperature difference depends on the natural air currents in a room. While most room fire experiments are in quiescent atmospheres, buildings usually have considerable natural air flow. The causes of such flows include stack effect, wind effect, HVAC systems, toilet exhausts, kitchen exhausts, convection currents due to heat transfer, office machinery cooling fans, and motion of elevators. In buildings the initiation temperature difference could be much larger than the default discussed above. The computer simulations discussed later include runs with different initiation temperature differences to provide some understanding of the effect of upper layer initiation. However, the runs of this paper do not address the interaction of layer initiation and delays in fire gases reaching a room.

## 6. Computer Simulations

Smoke movement was simulated for an eight story building shown in figure 7 with floor to ceiling heights of 3 m (9.8 ft) and floor to floor heights of 5 m (16.4 ft). Each floor consisted of one room, and the building had one shaft. This shaft has a floor area of 1 m<sup>2</sup> (10.8 ft<sup>2</sup>), and each floor has a floor area of 100 m<sup>2</sup> (1080 ft<sup>2</sup>). This building was selected to provide insight into simulating smoke flow in multi-story buildings, but it is realized that such simple buildings are not common.

The flow areas for the simulations are listed in table 1. Computer runs were made for a winter outside temperature of -17°C (1°F), a summer outside temperature of 37°C (90°F), initial conditions of zero flow and HVAC heating, and one and two zone shaft models. The conditions of the computer runs are listed in table 2. For these runs, the interface heights, temperatures and CO concentrations are shown in figures 8 through 42. These figures are arranged in the order in which the runs were made to aid readers looking for specific data. However, in the following sections some of the runs are discussed out of order so that similar topics can be grouped together.

### 6.1 Effect of HVAC Heating Without a Fire

Runs 1 and 2 are for winter outside temperature without a fire. Run 1 was with the zero flow initial condition, and run 2 was with HVAC heating. The purposes of these runs are to confirm the computer code modifications for HVAC heating and to show temperature transients within the building without HVAC heating.

As expected for run 1, the temperatures in building spaces decreased, and this is shown in figure 8 for the shaft and floors 1 and 8. The temperatures of other spaces were calculated in run 1. Only values at



Table 1. Building flow areas for runs with modified zone model

Flow Areas:	Height*		Area	
	m	ft	m <sup>2</sup>	ft <sup>2</sup>
Between Shaft and Typical Floor (for all runs except runs 13, 14 and 15)	2	6.6	0.02	0.22
Between Shaft and Typical Floor (for runs 13, 14 and 15)	2	6.6	0.20	2.2
Between Outside and Typical Floor	2	6.6	0.02	0.22
Between Outside and Shaft	40	131	2.0	22.
Between Outside and Floor 1	2	6.6	2.0	22.
Between Outside and Floor 3 (Runs 10, 11 and 12)	2	6.6	0.20	2.2

\*This height is the elevation above the floor level. All flow areas are gaps of constant width extending from the bottom of the space to this height.

these locations were plotted, to provide understanding of the main trends. This approach is used for presentation of the rest of the simulations. Calculations were made for all building locations, but only a few are presented to give the main trends.

Because there was no fire or other source of high temperature flow, no upper layers were established in any building spaces for run 1. Over the half hour simulation of run 1, the temperature of the first floor dropped to about -16°C (3°F). This was due to the flow of outside air, which was due to the large opening on that floor. This temperature change of 37°C (67°F) is significant for comfort and tenability but is small compared to the temperature changes due to fires. With HVAC heating (run 2) temperatures throughout the building were unchanged for the half hour simulation as shown in figure 8.

Runs 6 and 7 are the same as runs 1 and 2, except that runs 6 and 7 are for the summer outside temperature. As expected, the temperatures rise in run 6 due to inflow of hot outside air (figure 18). The temperatures of run 7 remain constant due to HVAC heating.

Runs 2 and 7 confirm the computer code modifications for HVAC heating. Runs 1 and 6 show that without both a fire and HVAC heating, the temperatures within the building move towards the outside temperature.

Table 2. Conditions of runs with modified zone model

Run *	Outside Temperature		Initial Conditions **	Shaft Model	Fire Size MW	Fire Floor
	°C	°F				
1	-17	1	0 Flow	2 Zone	none	-
2	-17	1	HVAC	1 Zone	none	-
3	-17	1	0 Flow	2 Zone	2	1
4	-17	1	HVAC	2 Zone	2	1
5	-17	1	HVAC	1 Zone	2	1
6	37	99	0 Flow	2 Zone	none	-
7	37	99	HVAC	1 Zone	none	-
8	37	99	0 Flow	2 Zone	2	1
9	37	99	HVAC	2 Zone	2	1
10	37	99	0 Flow	2 Zone	2	3
11	37	99	HVAC	2 Zone	2	3
12	37	99	HVAC	1 Zone	2	3
13	-17	1	0 Flow	2 Zone	2	1
14	-17	1	HVAC	2 Zone	2	1
15	-17	1	HVAC	1 Zone	2	1
16	37	99	0 Flow	2 Zone	none	-
17	37	99	HVAC	1 Zone	2	3
18	-17	1	HVAC	1 Zone	2	1

\*Runs 1 to 15 were made with a layer initiation temperature difference of 40°C (72°F), and runs 16, 17 and 18 made with a layer initiation temperature difference of 1°C (1.8°F).

\*\*Initial conditions: 0 Flow is zero mass flow at a constant temperature of 21°C (70°F) for all building spaces, and HVAC is steady mass flow with simulated HVAC heating to maintain that steady flow in the absence of a fire.

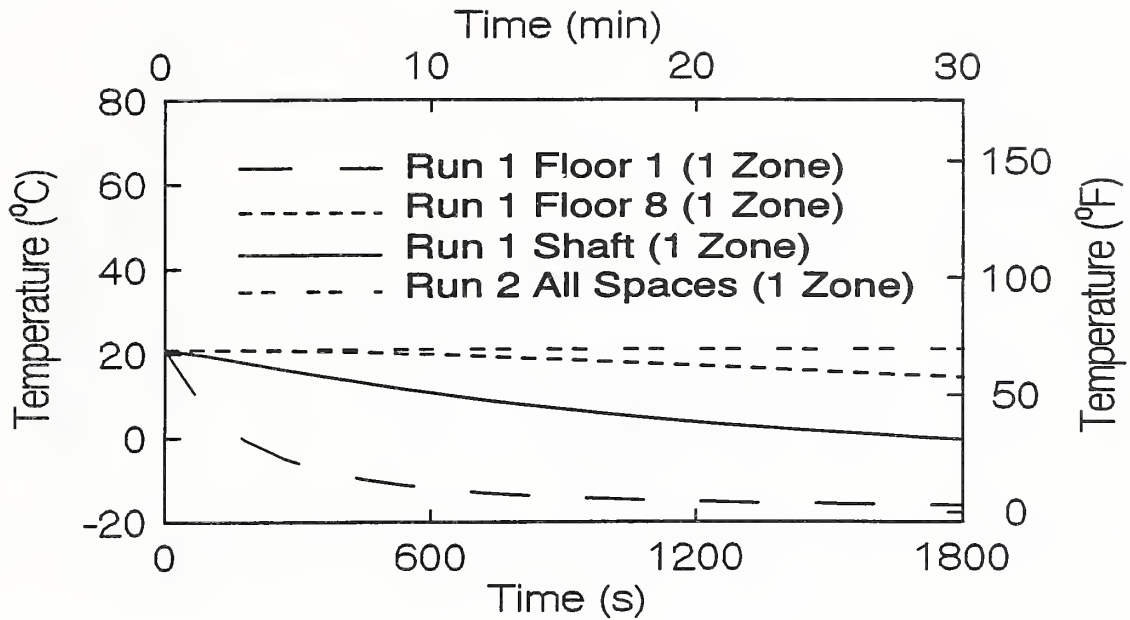


Figure 8. Temperatures from runs 1 and 2

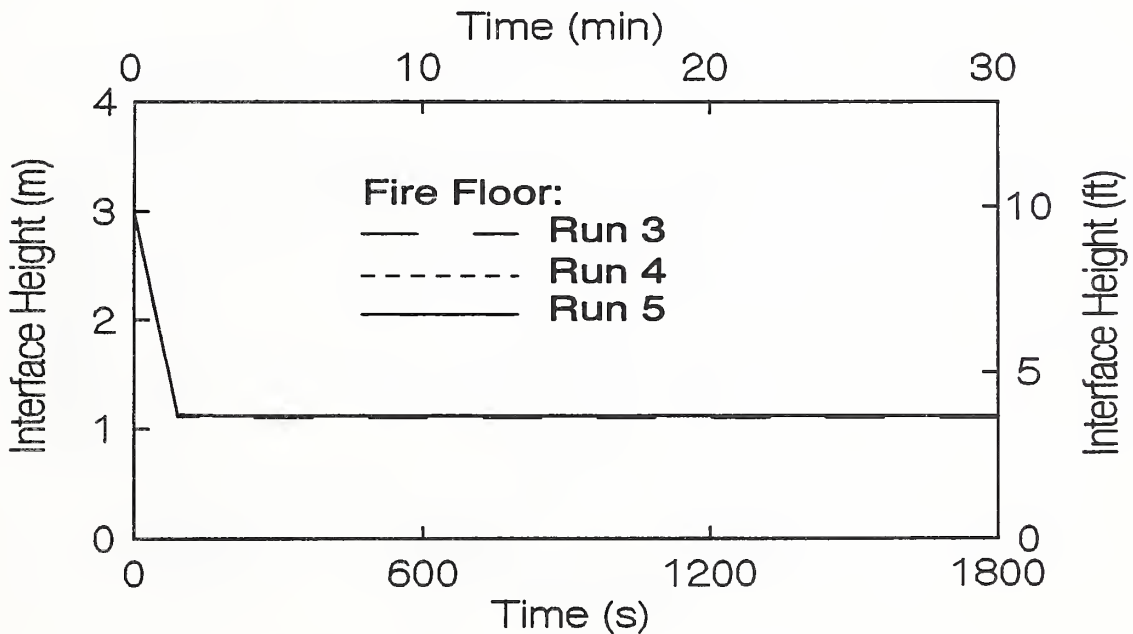


Figure 9. Interface heights on fire floor (floor 1) for runs 3, 4 and 5

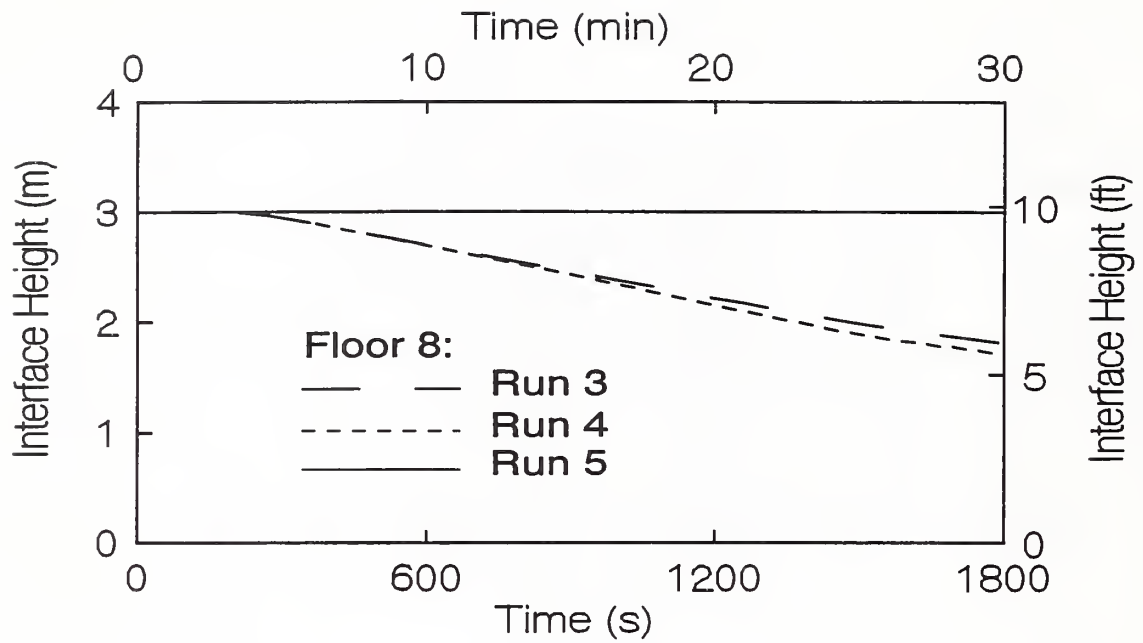


Figure 10. Interface heights on floor 8 for runs 3, 4 and 5

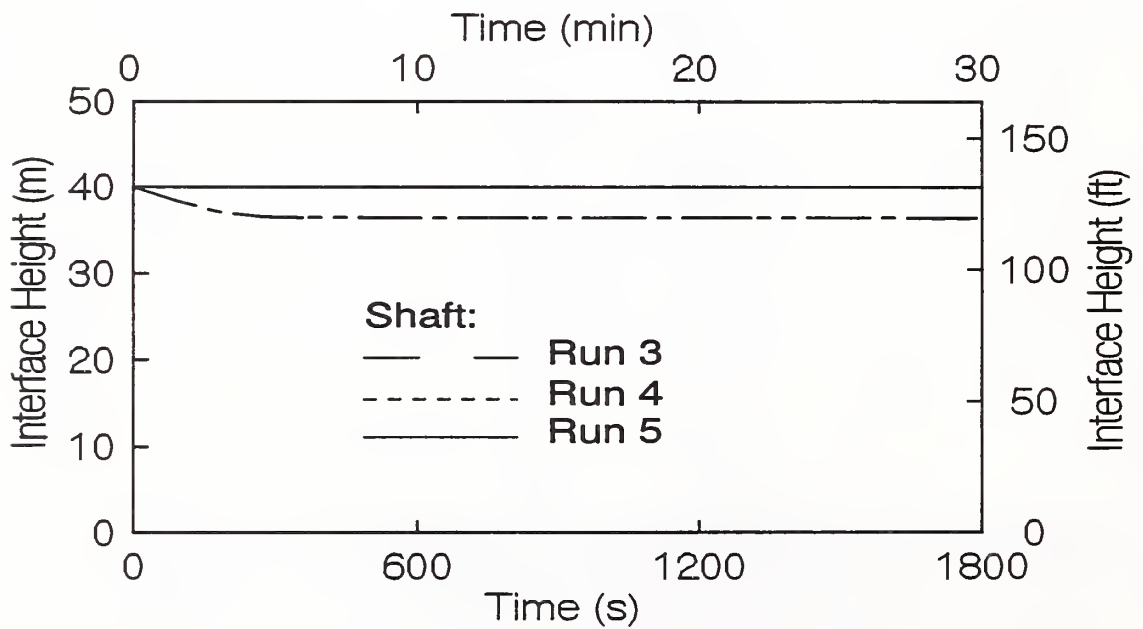


Figure 11. Interface height in shaft for runs 3, 4 and 5



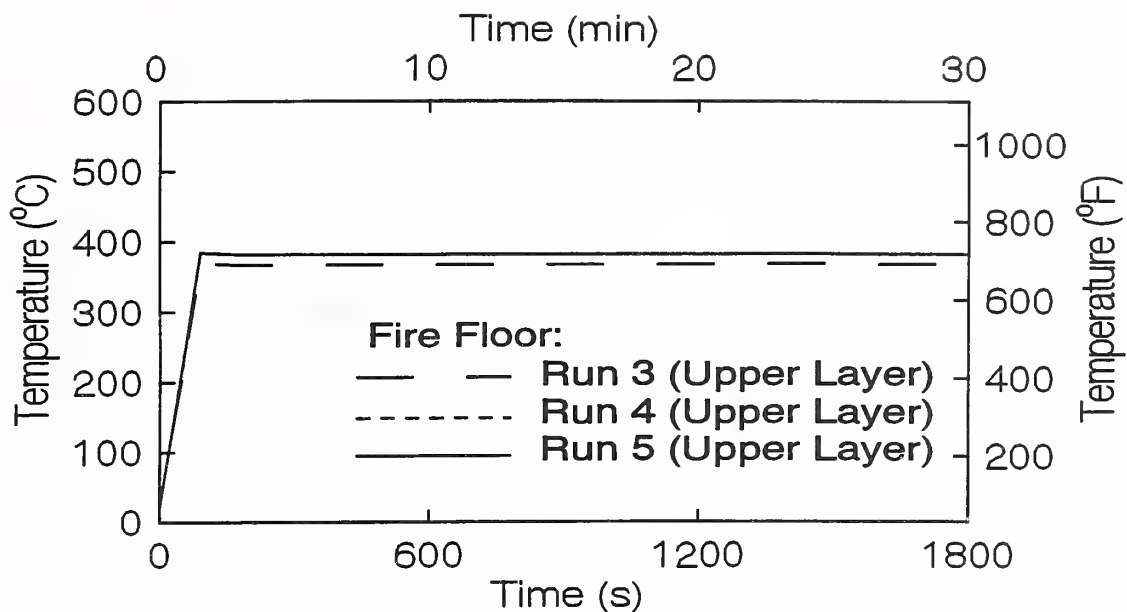


Figure 12. Temperature on fire floor (floor 1) for runs 3, 4 and 5

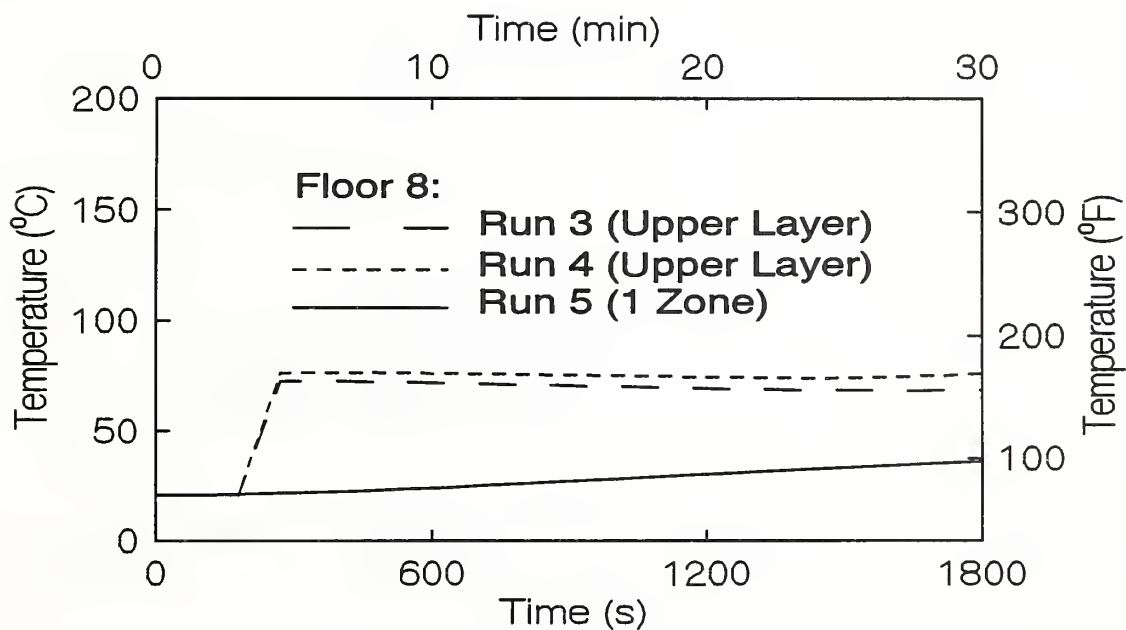


Figure 13. Temperature on floor 8 for runs 3, 4 and 5

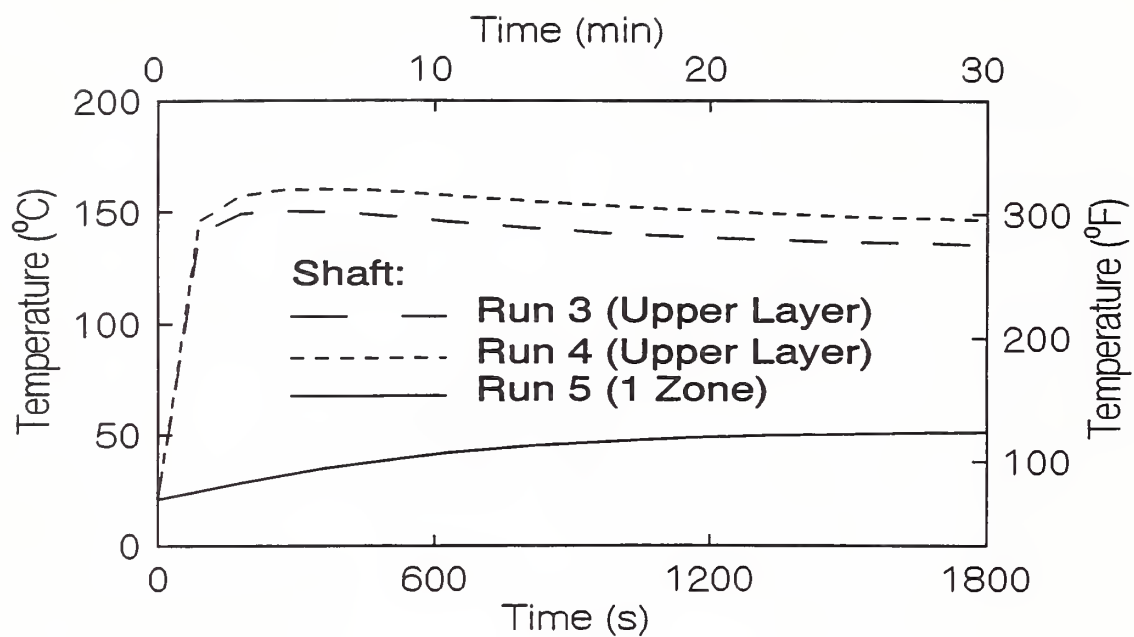


Figure 14. Temperature in shaft for runs 3, 4 and 5

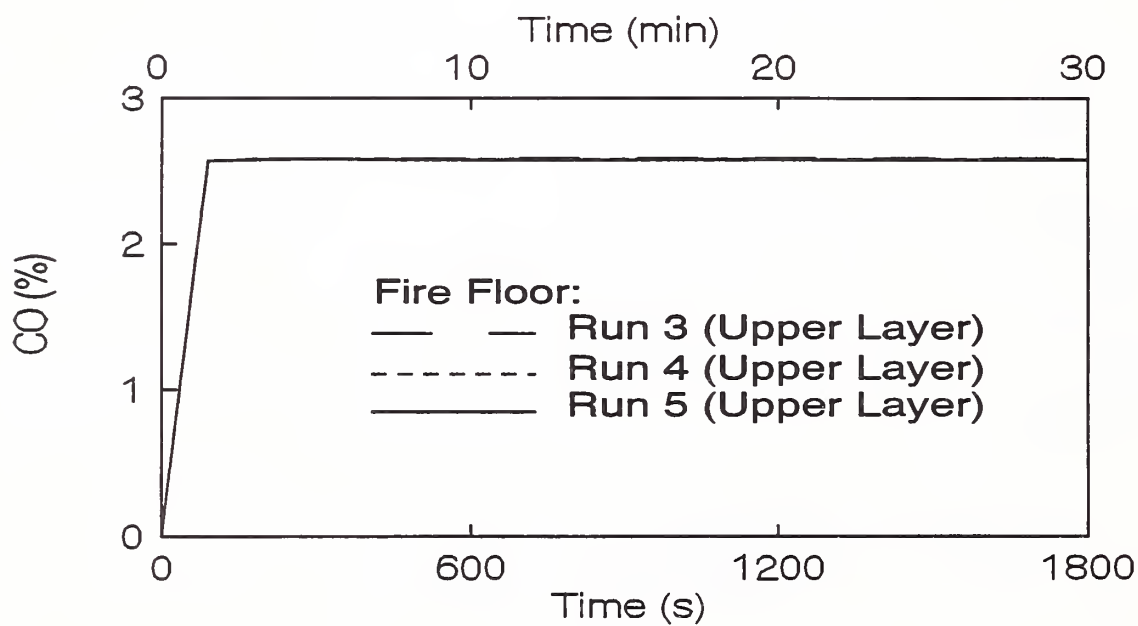


Figure 15. CO concentration on fire floor (floor 1) for runs 3, 4 and 5

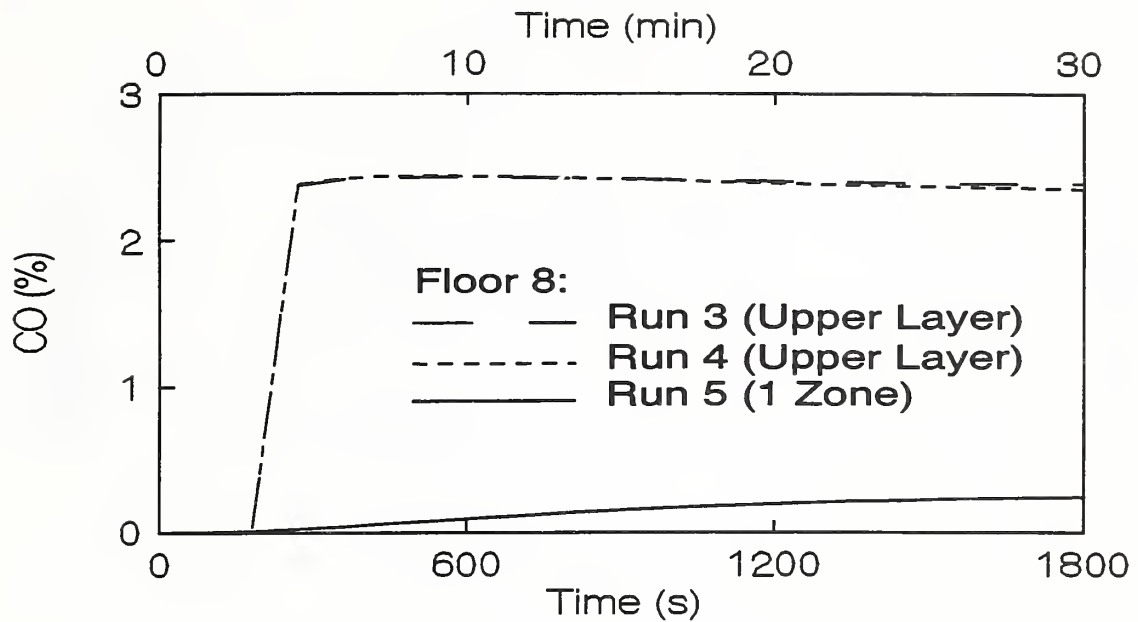


Figure 16. CO concentration on floor 8 for runs 3, 4 and 5

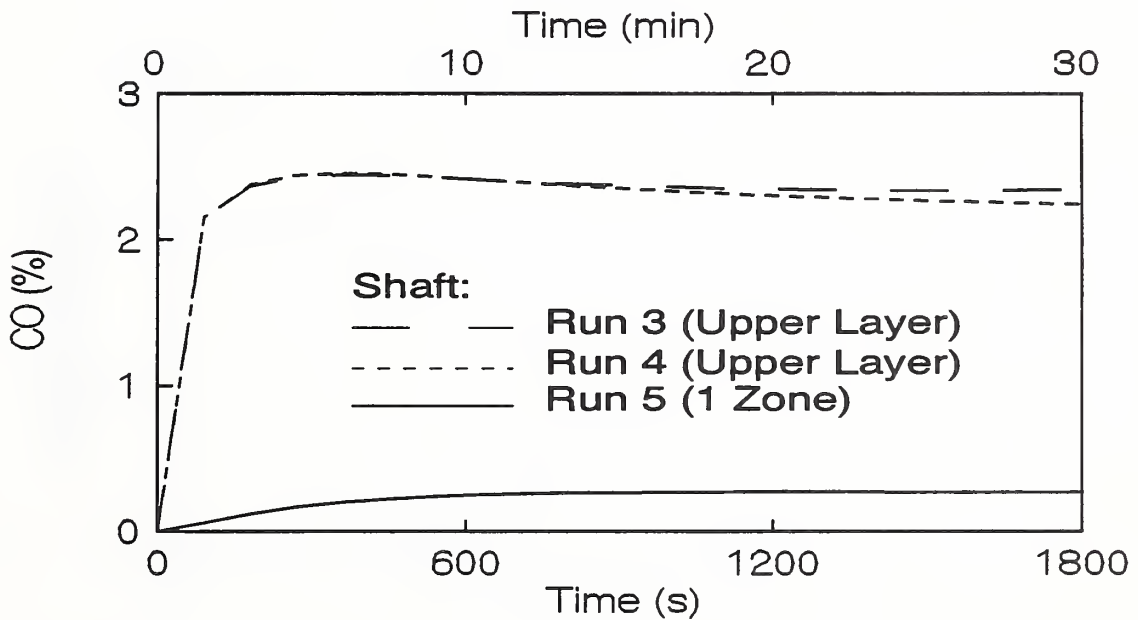


Figure 17. CO concentration in shaft for runs 3, 4 and 5

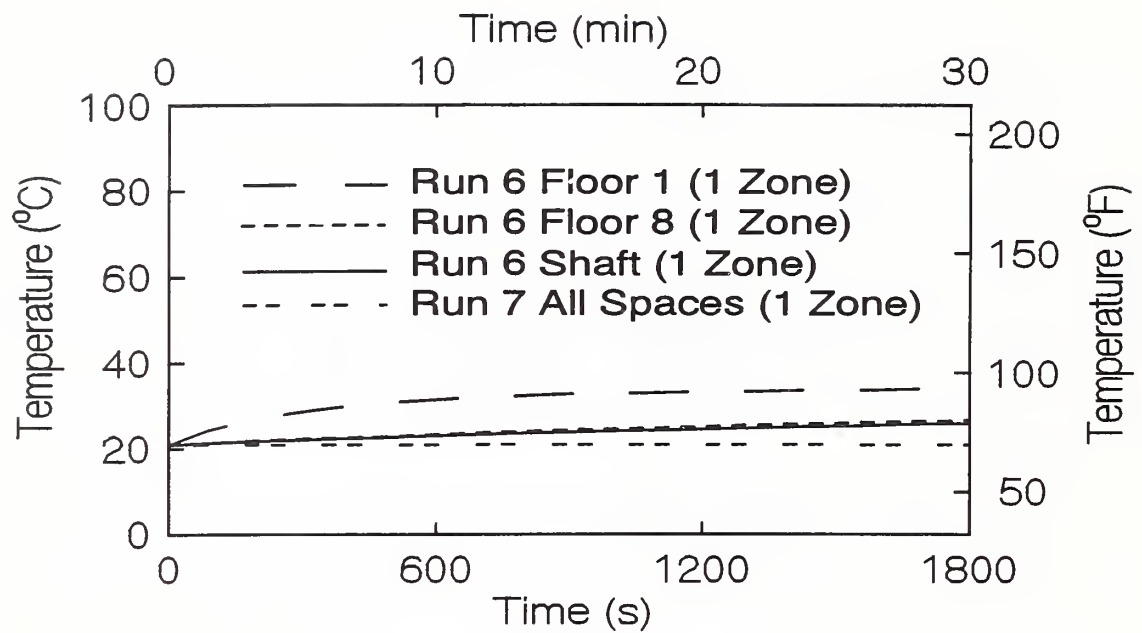


Figure 18. Temperatures from runs 6 and 7

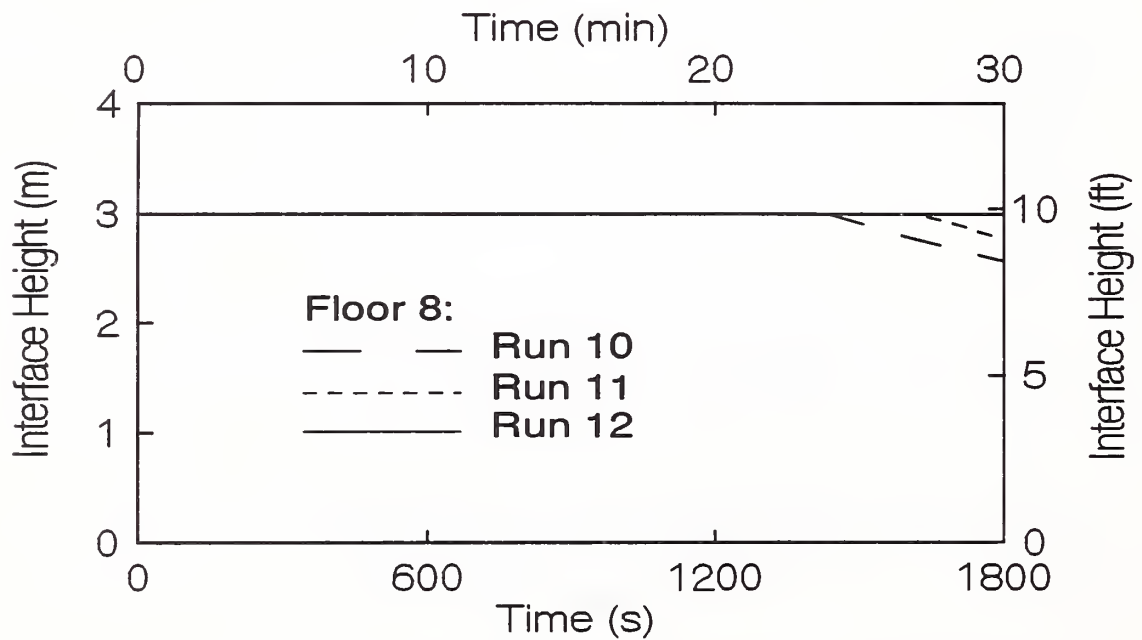


Figure 19. Interface heights on floor 8 for runs 10, 11 and 12

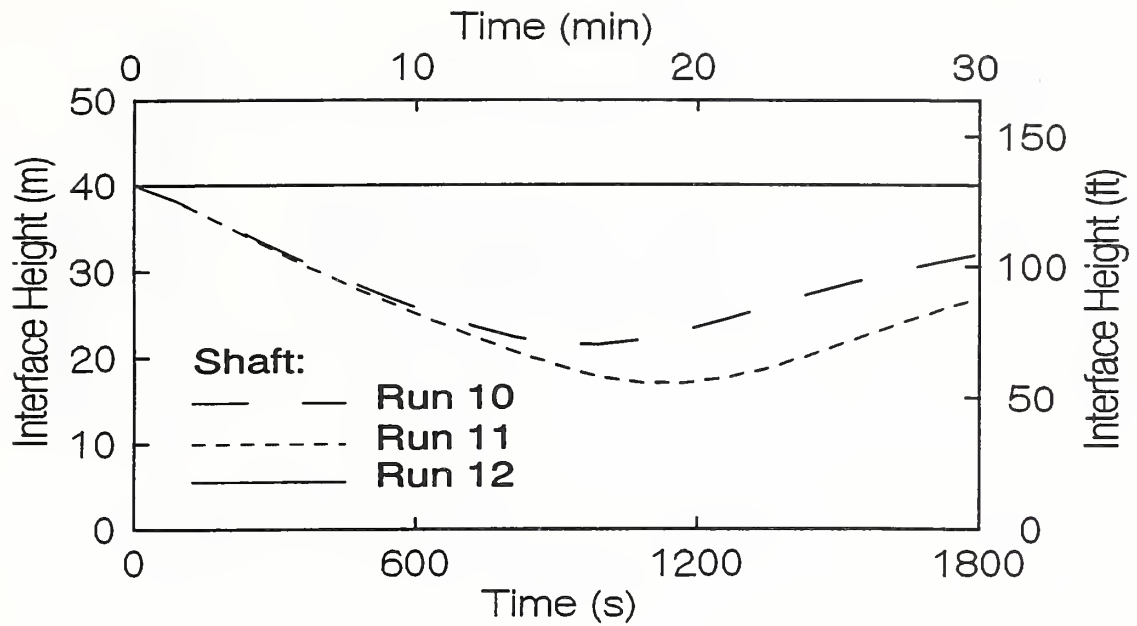


Figure 20. Interface height in shaft for runs 10, 11 and 12

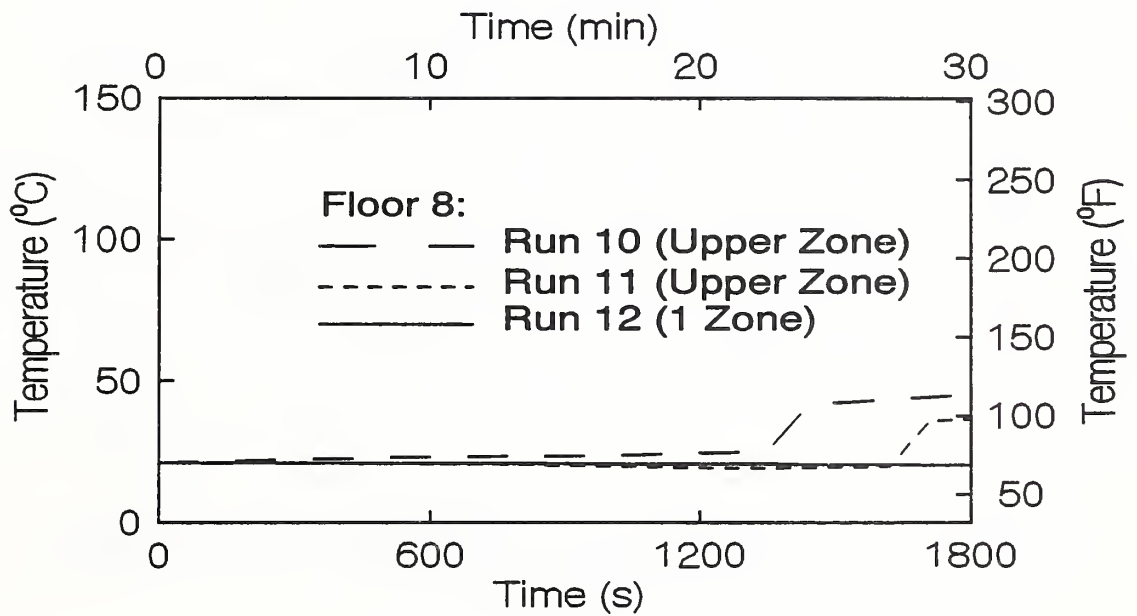


Figure 21. Temperature on floor 8 for runs 10, 11 and 12

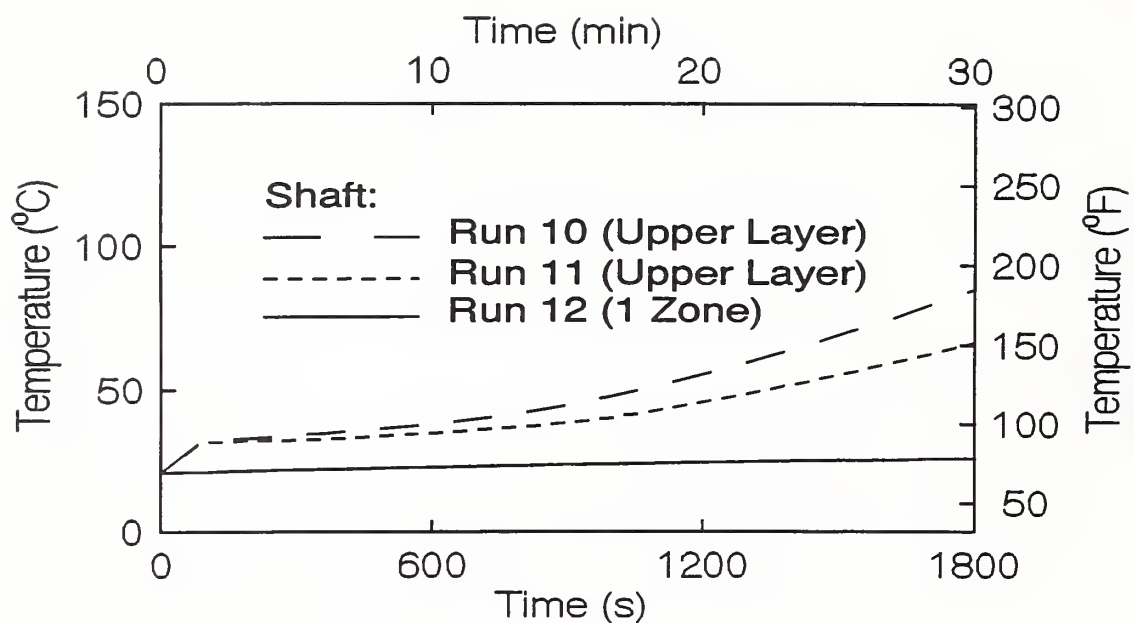


Figure 22. Temperature in shaft for runs 10, 11 and 12

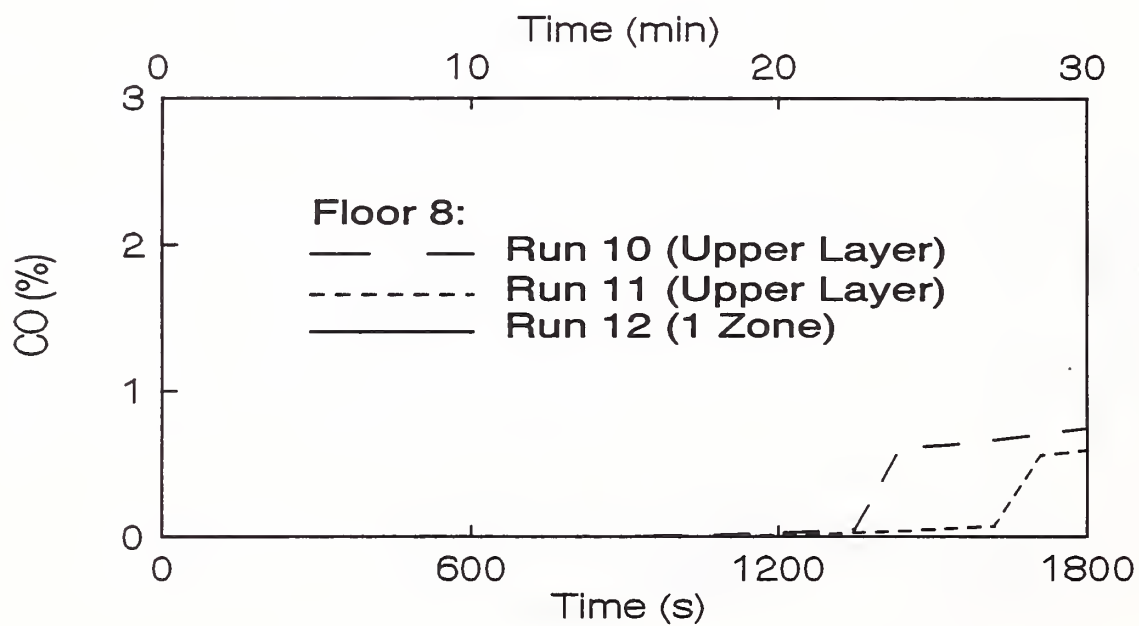


Figure 23. CO concentration on floor 8 for runs 10, 11 and 12

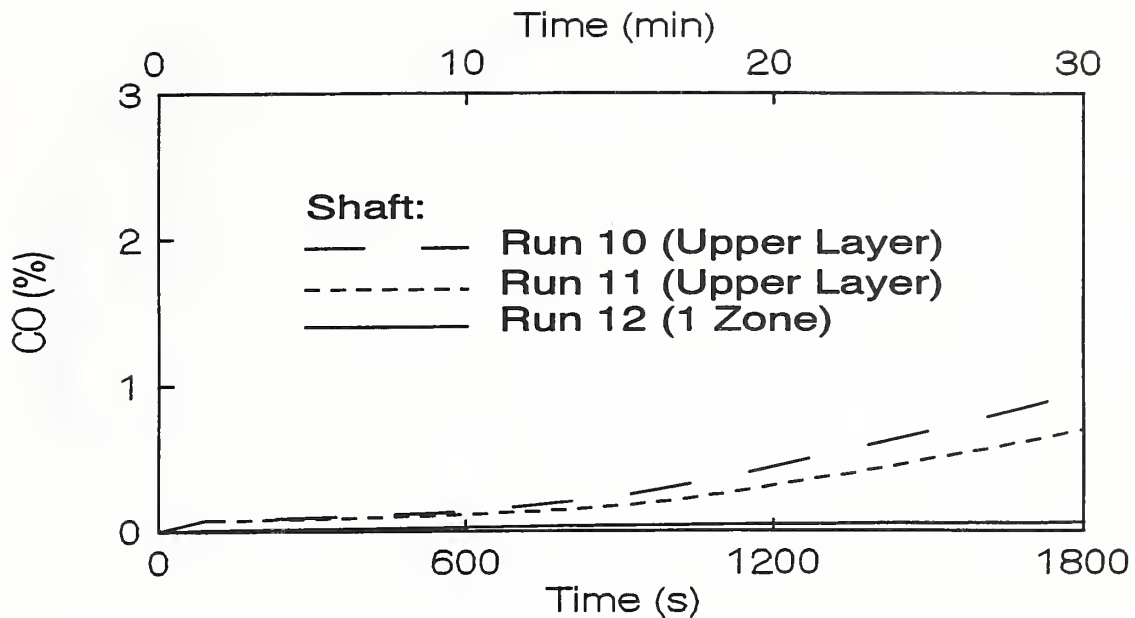


Figure 24. CO concentration in shaft for runs 10, 11 and 12

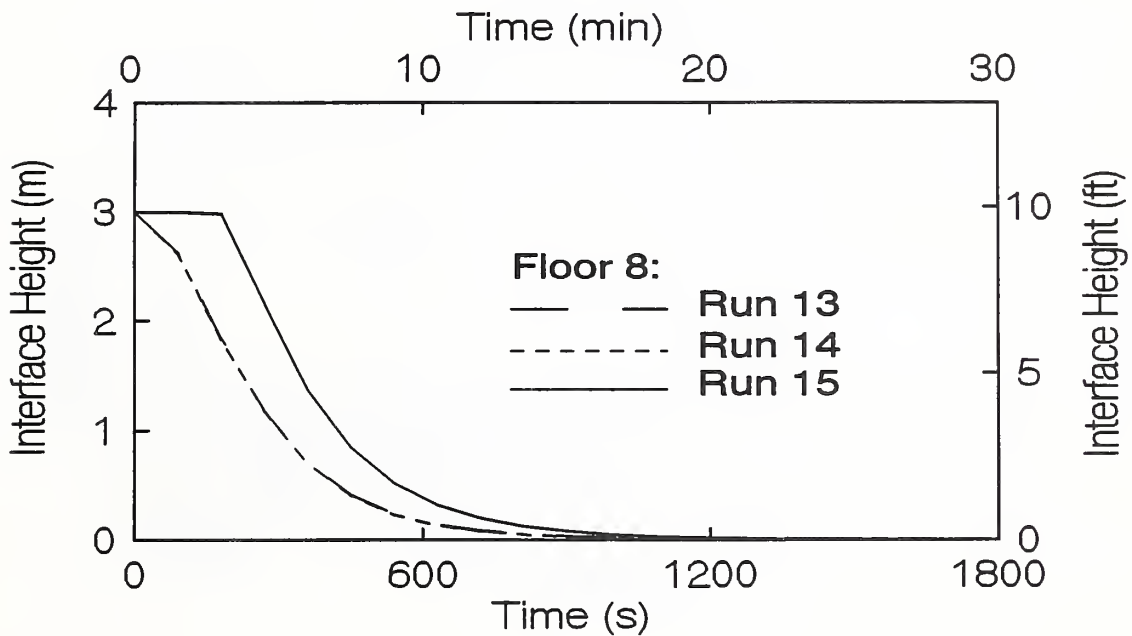


Figure 25. Interface heights on floor 8 for runs 13, 14 and 15

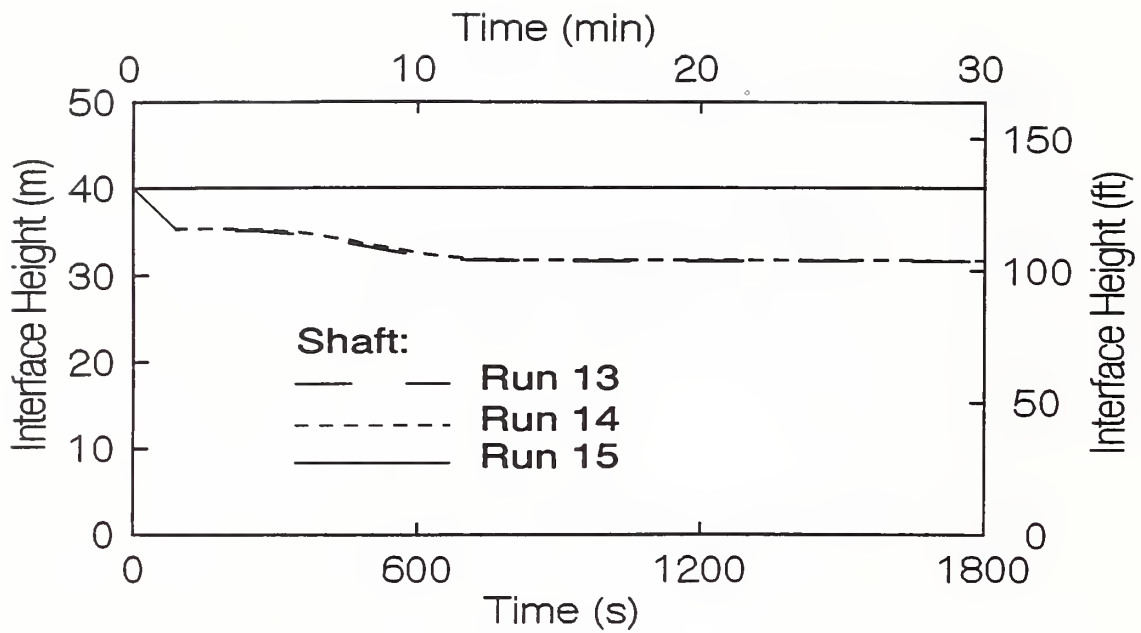


Figure 26. Interface height in shaft for runs 13, 14 and 15

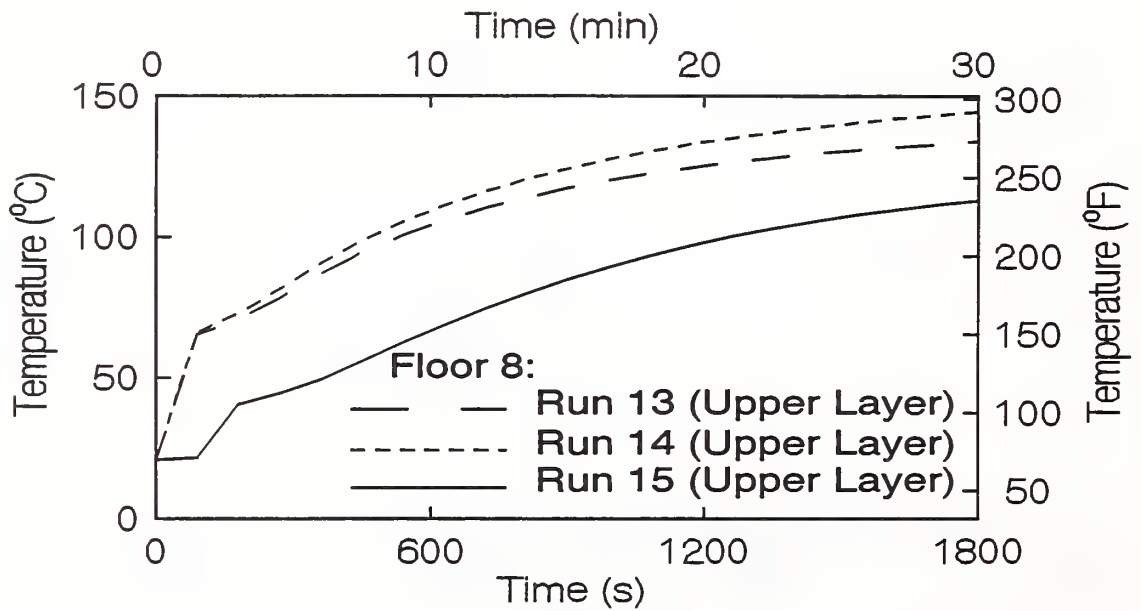


Figure 27. Temperature on floor 8 for runs 13, 14 and 15



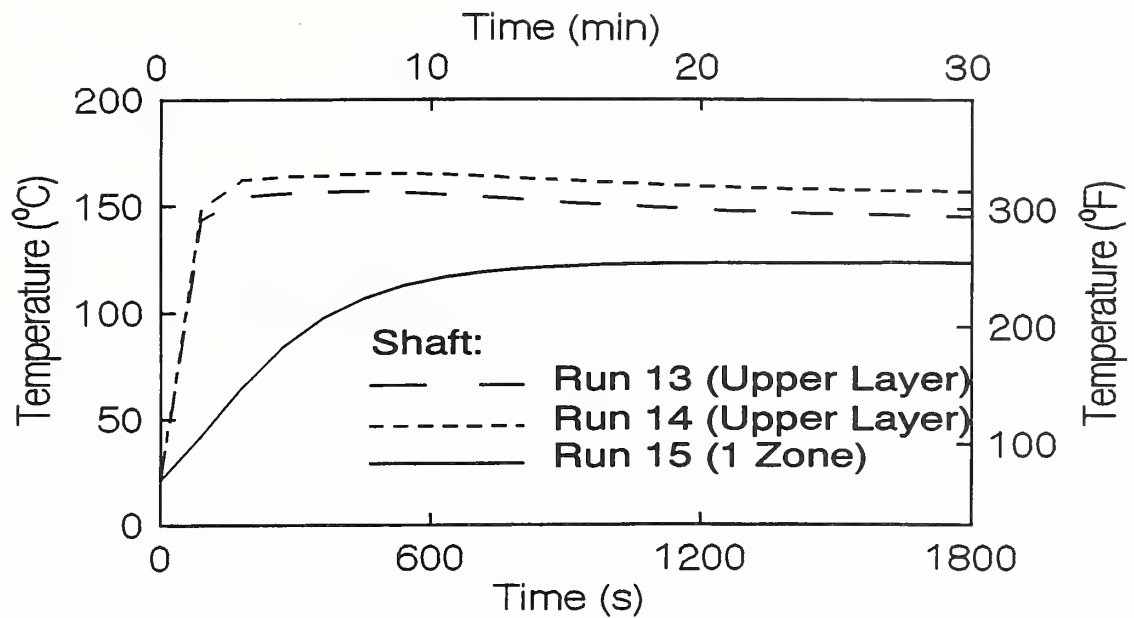


Figure 28. Temperature in shaft for runs 13, 14 and 15

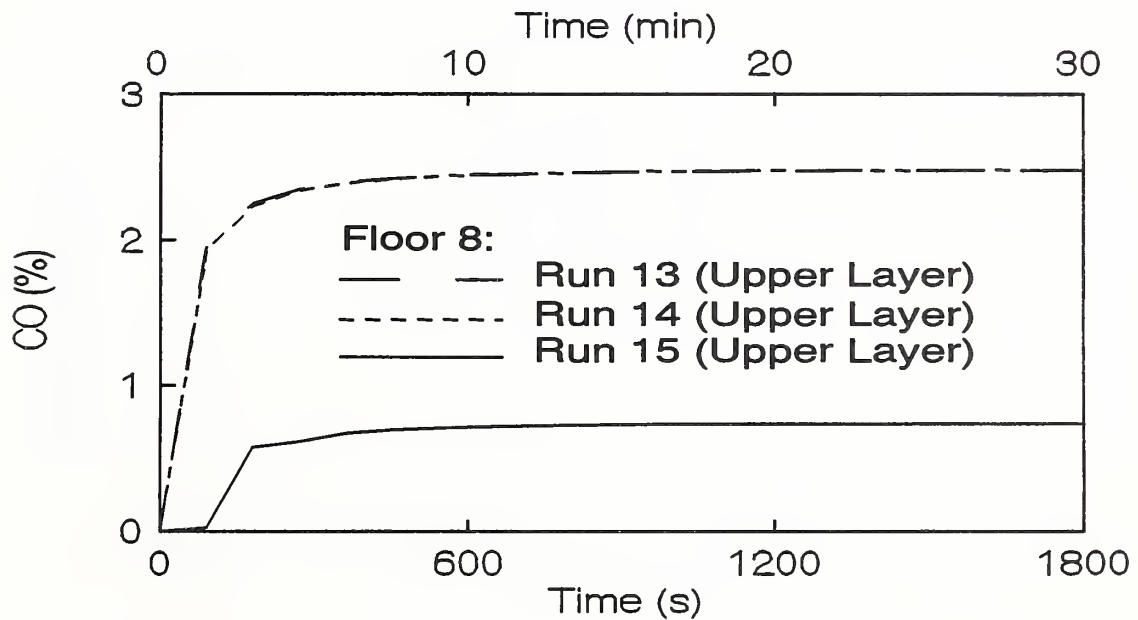


Figure 29. CO concentration on floor 8 for runs 13, 14 and 15

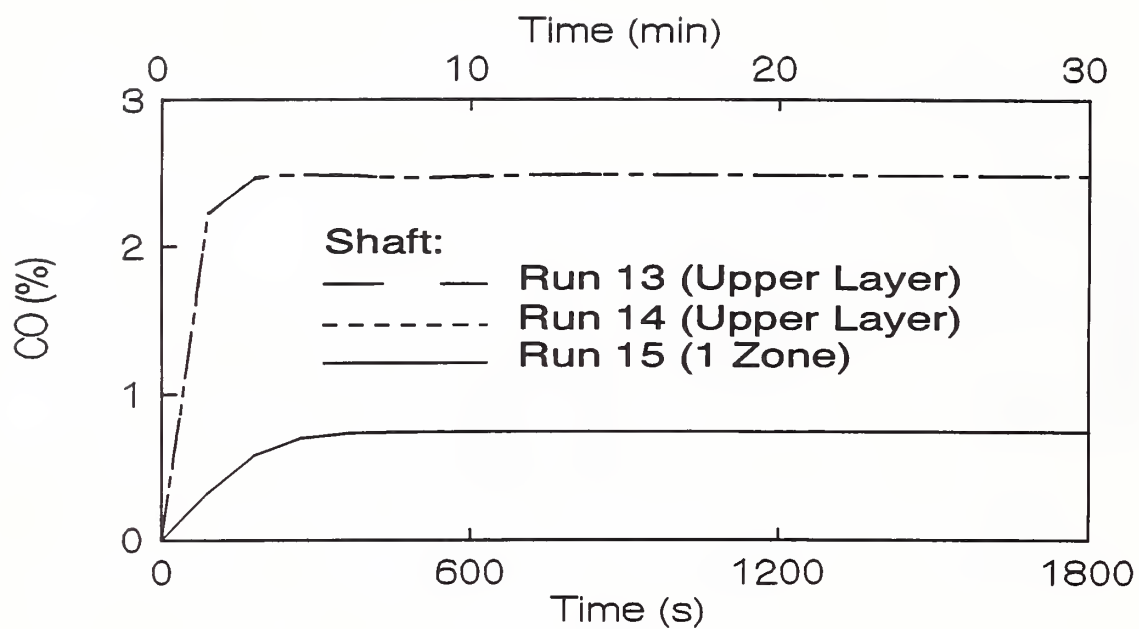


Figure 30. CO concentration in shaft for runs 13, 14 and 15

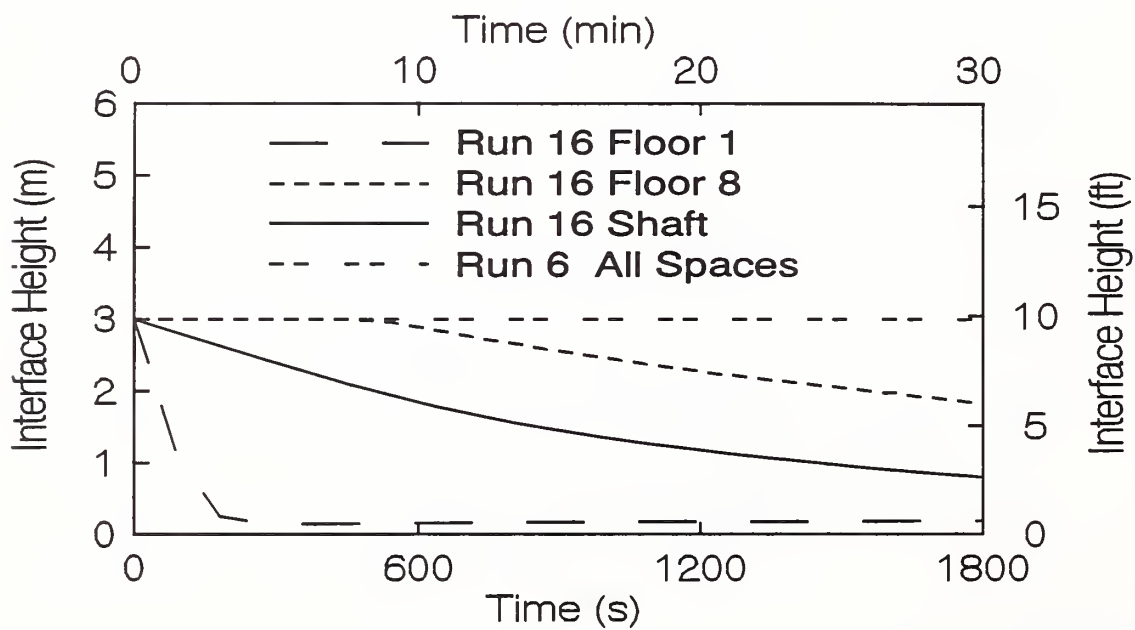


Figure 31. Interface Heights for runs 6 and 16

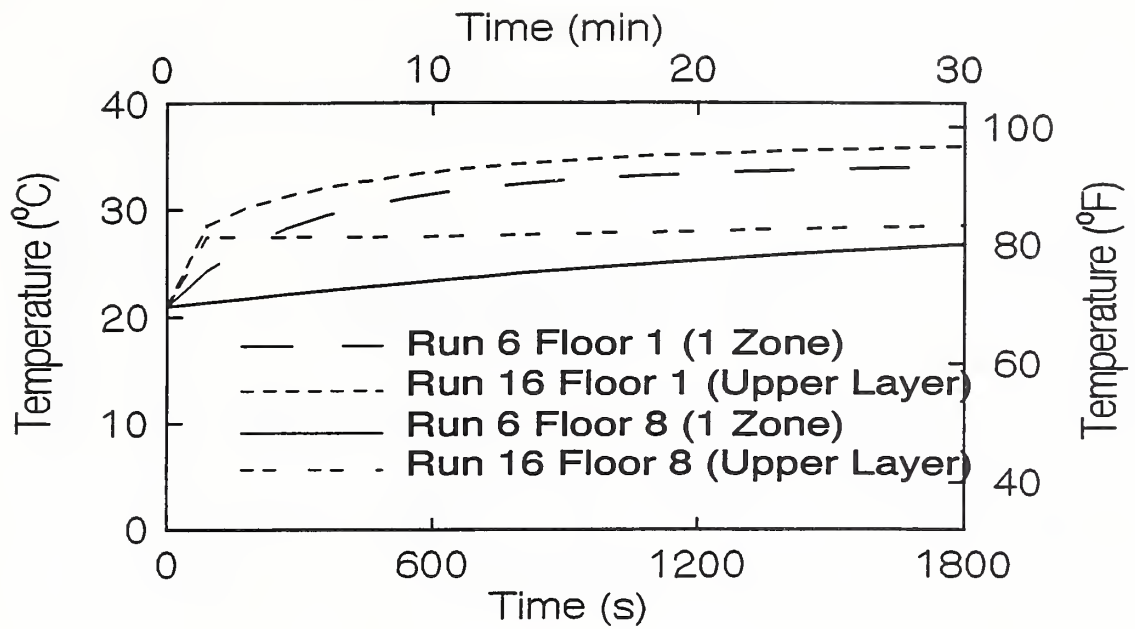


Figure 32. Temperatures for runs 6 and 16

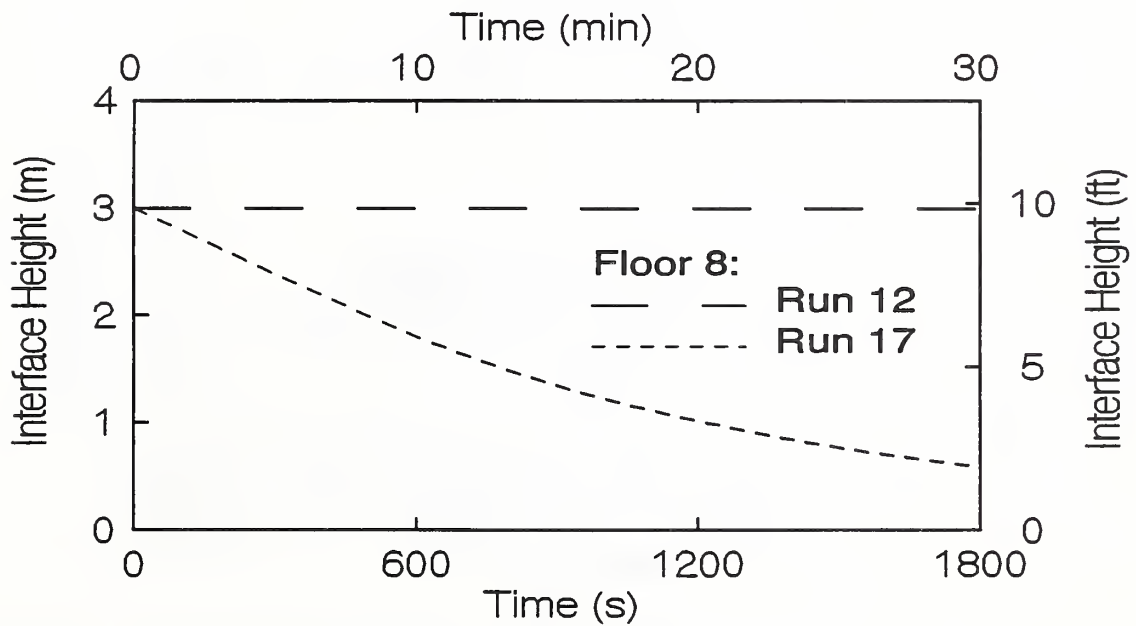


Figure 33. Interface heights on floor 8 for runs 12 and 17

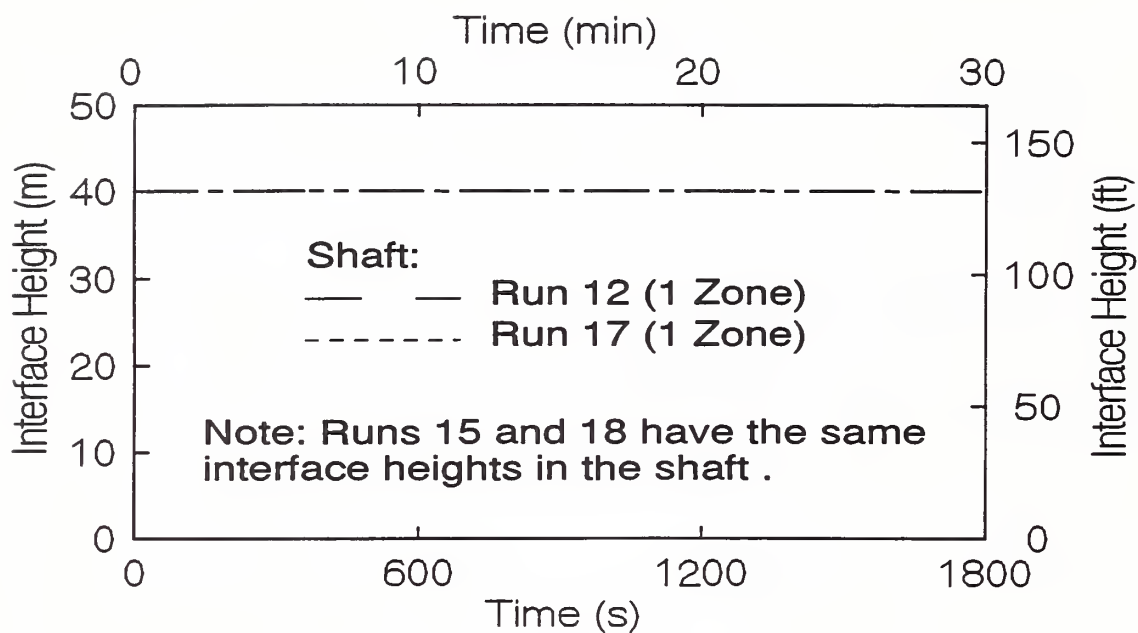


Figure 34. Interface height in shaft for runs 12 and 17

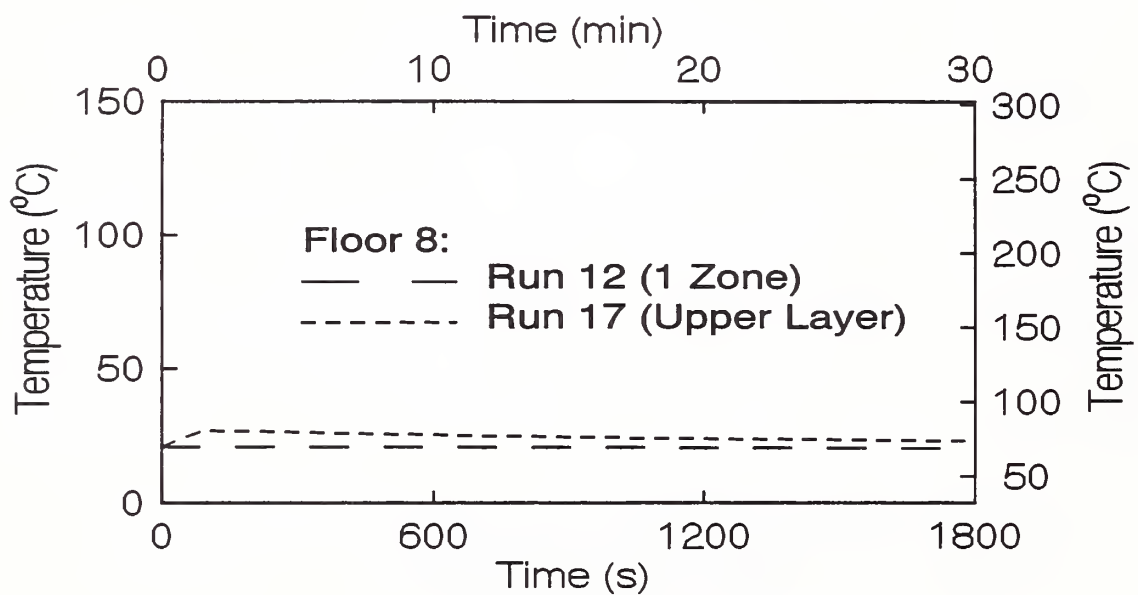


Figure 35. Temperature on floor 8 for runs 12 and 17

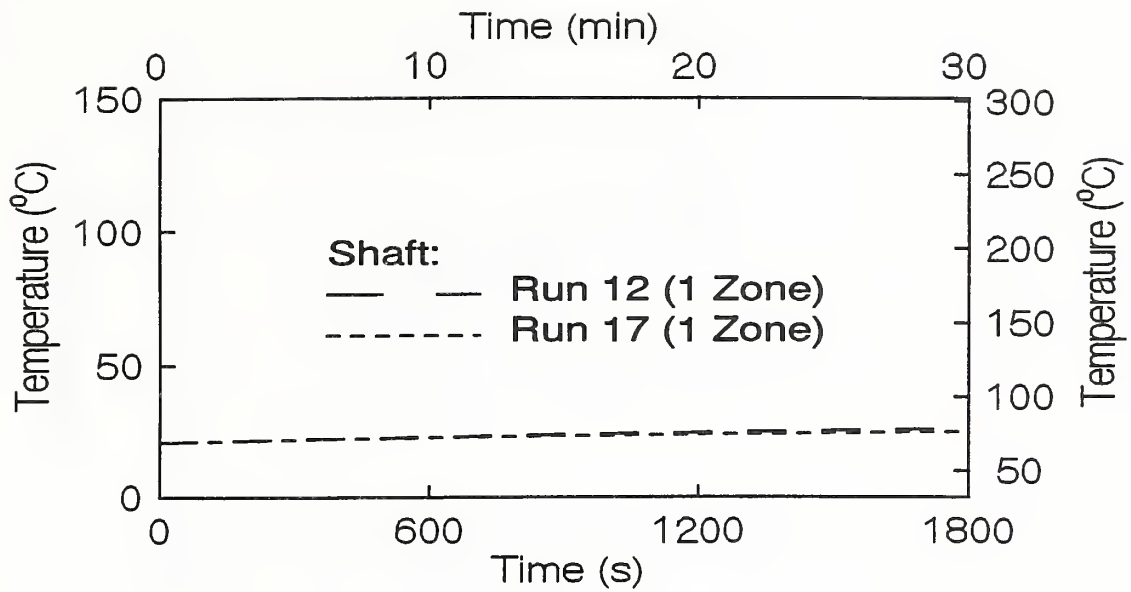


Figure 36. Temperature in shaft for runs 12 and 17

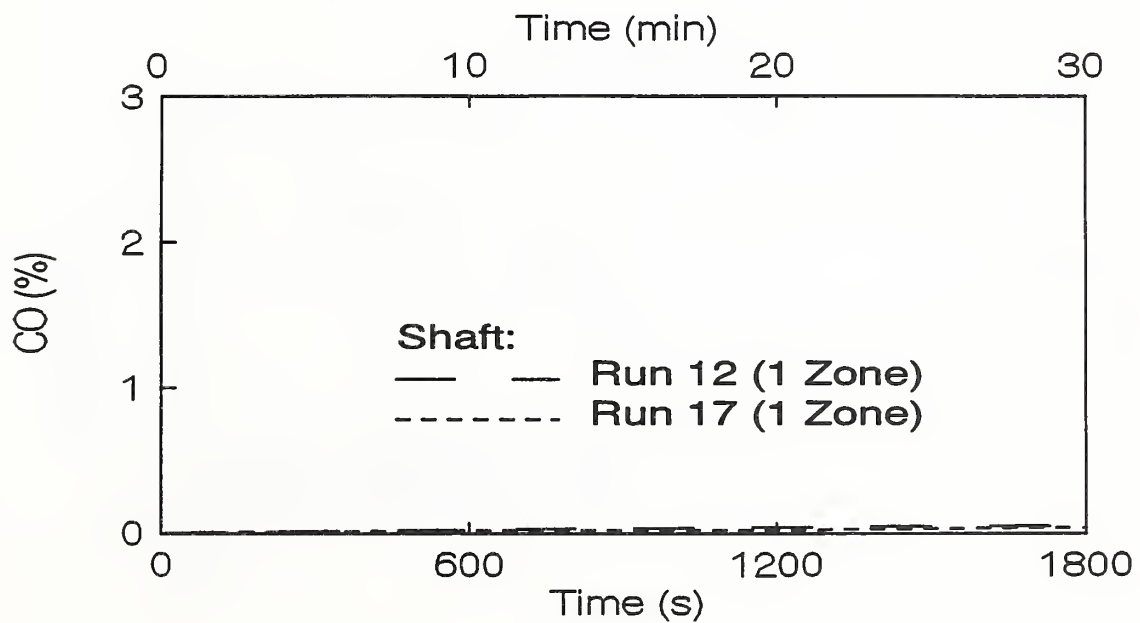


Figure 37. CO concentration in shaft for runs 12 and 17

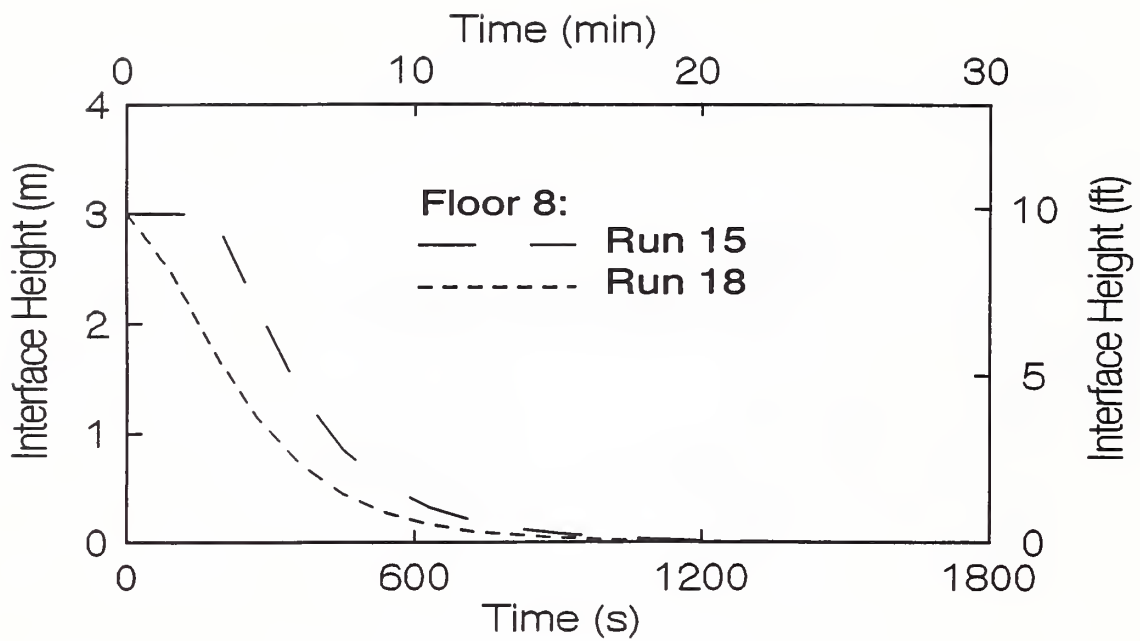


Figure 38. Interface heights on floor 8 for runs 15 and 18

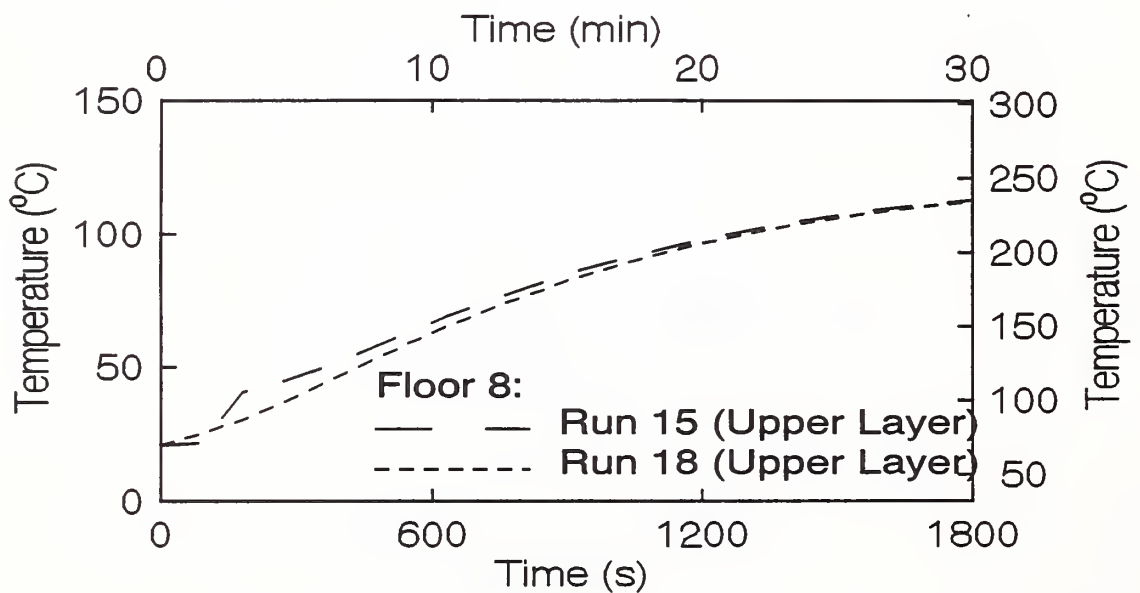


Figure 39. Temperature on floor 8 for runs 15 and 18

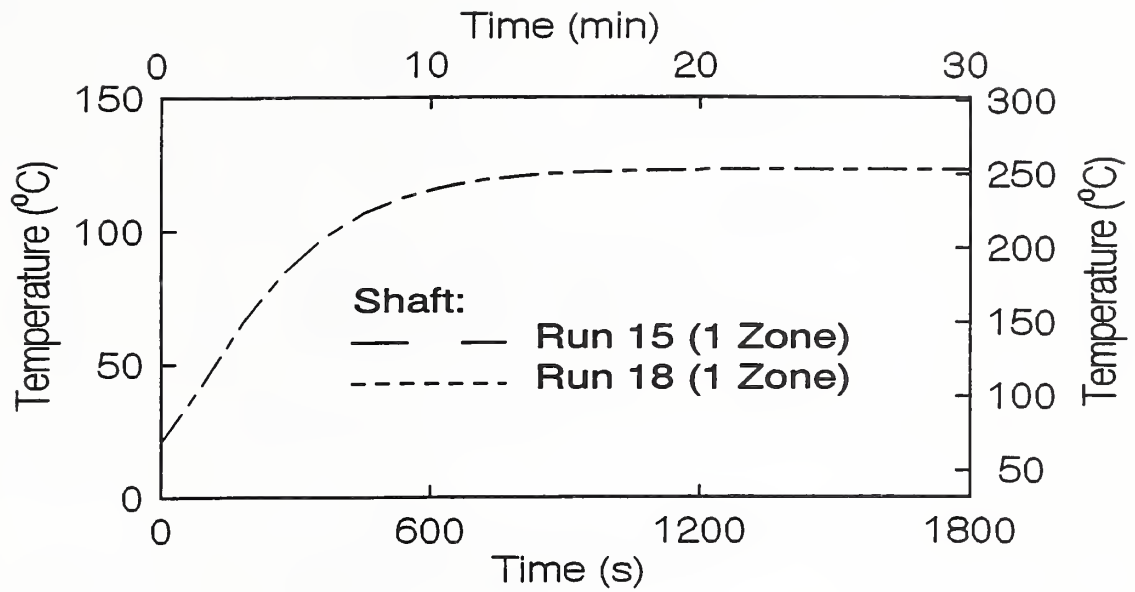


Figure 40. Temperature in shaft for runs 15 and 18

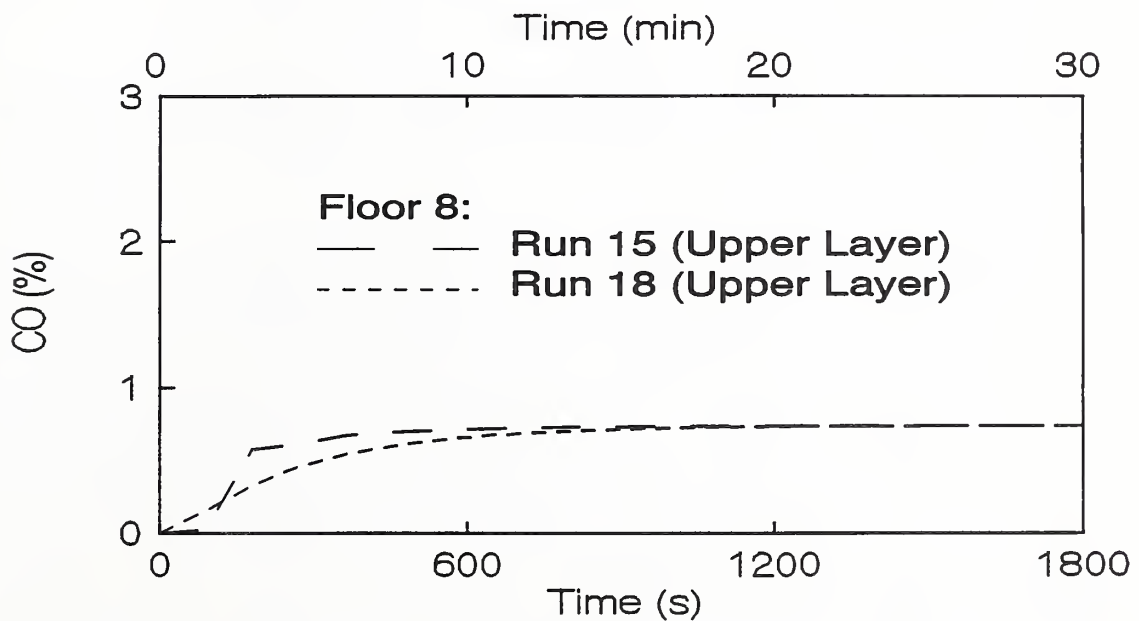


Figure 41. CO concentration on floor 8 for runs 15 and 18

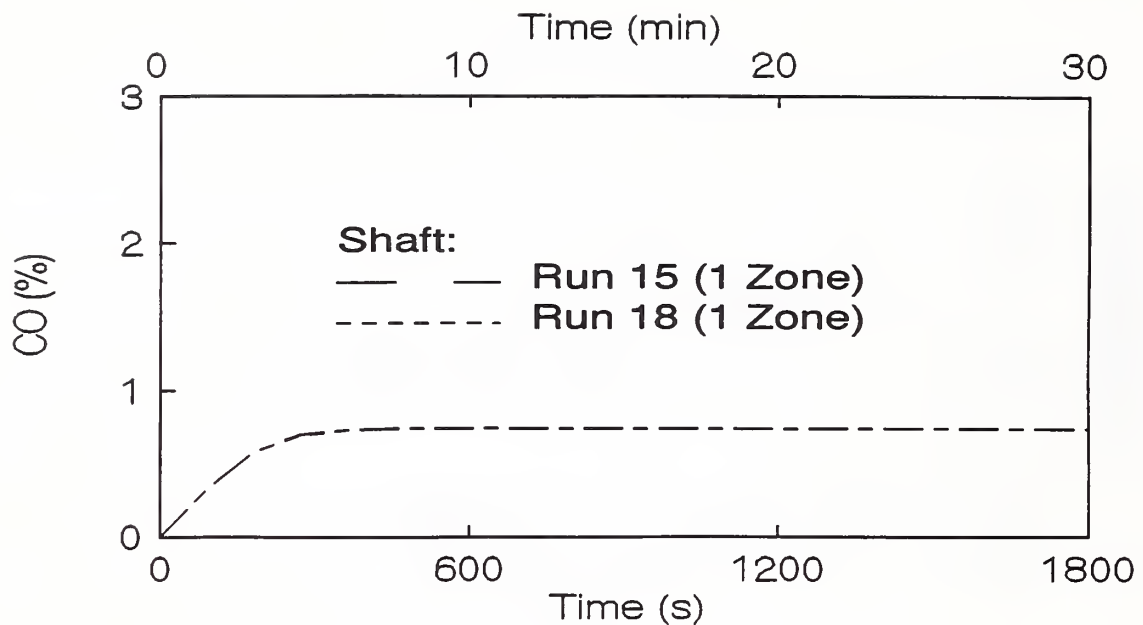


Figure 42. CO concentration in shaft for runs 15 and 18

## 6.2 First Floor Fire and Normal Stack Effect

Runs 3, 4 and 5 are with a 2 MW fire on the first floor during outside winter temperatures. The purposes of these runs are to show the effect of HVAC heating and to show the difference between the one and two zone shaft model during normal stack effect.

Examination of figure 9 shows that HVAC heating and the type of shaft model have only a slight effect on the interface height on the fire floor. The range of interface heights amounts to only about 3%. Further, figure 12 shows that HVAC heating and the type of shaft model have only a small effect on the upper layer temperature on the fire floor. The upper layer fire floor temperatures are the same for the two runs (4 and 5) with HVAC heating. Without HVAC heating (run 3) the temperature at this location is about 10°C (18°F) lower. This is probably because the HVAC heating adds heat to the fire floor. However, this may not happen during many fires, because the heating may be shut off upon fire detection or the heating may be damaged by the fire. The CO concentrations of the upper layer of the fire floor for these runs (3, 4 and 5) were all 2.6% as shown in figure 15. CO concentrations were calculated by the zone fire model as a constant CO production per kW of heat release, and this rate was intentionally chosen to give high CO concentrations on the fire floor. Thus for these runs, both HVAC heating and the shaft model have only a slight effect of the interface height, the upper layer temperature or CO concentration on the fire floor.

For all of the other runs with fires, the effect of HVAC heating and the shaft model are also slight. Also for these other runs, the shape of the curves for interface height, upper layer temperature and CO on the



fire floor are all similar to the curves for runs 3, 4 and 5 (figures 9, 12 and 15). In all these curves, the parameters reach a steady value in about 30 seconds. For a zone model with more detailed heat transfer, the time to reach steady fire floor conditions may be longer. Because these fire floor conditions are so similar, no figures of them are presented for the other runs, but the steady values of fire floor temperature and CO concentration are listed in table 3 for all simulations which included fires. Comparison of these steady values and the conditions of the runs (table 2) support the conclusion that neither HVAC heating or the shaft model have any significant effect on fire floor conditions.

Examination of figures 11, 14 and 17 show that the shaft model has significant impact on simulated conditions in shaft. For the two zone shaft model (runs 3 and 4), the interface height in the shaft is about 37 m (120 ft), the upper layer temperature reaches about 150°C (300°F), and the upper layer CO concentration reaches about 0.24%. For the one zone shaft model (run 3), there is no upper layer, the lower layer reaches about 50°C (120°F) with about 0.23% CO.

The shaft model has a significant impact on the simulated conditions on the eighth floor as can be seen from figures 10, 13 and 16. For the two zone model (run 3 and 4), the interface height drops to about 1.8 m (6 ft), the upper layer temperature reaches about 70°C (160°F), and the upper layer CO reaches about 2.4%. With the one zone model, no upper layer is formed and the lower layer reaches about 35°C (95°F) with about 0.20% CO. Examination of above referenced figures for these runs shows that HVAC heating had only slight impact on conditions in the shaft and on floor 8.

The conditions both in the shaft and on floor are significantly different for the two types of shaft models. For reasons previously stated, the two zone model is not appropriate for this shaft. Thus the two zone model can result in conditions in the shaft and on other floors that are unrealistic.

Table 3. Steady fire temperatures and CO concentrations

Run	Upper Layer Fire Floor Temperature*		Upper Layer Fire Floor CO**
	°C	°F	%
3	370	700	2.6
4	380	720	2.6
5	380	720	2.6
8	500	930	3.1
9	500	930	3.1
10	500	930	3.1
11	500	930	3.1
12	500	930	3.1
13	360	680	2.5
14	380	720	2.5
15	380	720	2.5
17	500	930	3.1
18	380	720	2.5

\*Upper zone fire floor temperature calculated by modified zone model.

\*\*Upper zone CO concentration calculated by modified zone model.

### 6.2.1 Large Flow Areas

Runs 13, 14 and 15 are the same as runs 3, 4 and 5, except that for the later runs the flow areas between the shaft and a typical floor were ten times greater than those of the earlier runs (table 1). The purpose of these runs was to see the impact of larger flow areas on the conditions in the shaft and on floor 8. Because of the inappropriateness of the two zone shaft model to this problem, the details of simulations with this model are not discussed. However, figures 25 to 30 show the results of these simulations along with those from the one zone model. It should be noted that for the runs of this section, the two zone shaft model results in similar errors to those of runs 3 and 4.

For the one zone shaft model, the large flow areas (run 15) result in shaft a temperature of about 130°C (270°F) (figure 28), and the small flow areas (run 5) result in a shaft temperature of about 50°C (120°F) (figure 14). With the large flow areas, the CO concentration in the shaft reaches about 0.46% (figure 30), which is twice the level (figure 17) for the small areas.

The larger flow areas resulted in very different conditions on floor 8 for run 15 as compared to run 5. For run 5, there was no upper layer on floor 8, and the lower layer reached about 35°C (95°F) (figure 13) with about 0.20% CO (figure 16). For run 15, the interface height went down to the floor (figure 25), and the upper layer reached about 120°C (250°F) (figure 27) and about 0.46% CO (figure 29).

### 6.3 First Floor Fire and Reverse Stack Effect

Runs 8 and 9 were similar to runs 3 and 4, except that they were made for the summer outside temperature. These runs were conducted to see the impact of reverse stack effect on smoke flow. Run 8 was without HVAC heating, and run 9 was with HVAC heating. For both runs, the pressures due to reverse stack effect prevented smoke infiltration into the shaft, and thus to other floors of the building. However, if the example building had leakage between the floors, smoke may have reached other floors through these paths.

The following approach can be used to estimate if reverse stack effect will prevent smoke flow into a shaft. If the pressure difference due to reverse stack effect is greater than that due fire gas buoyancy, smoke will not flow into the shaft. The pressure difference due to fire gas buoyancy is

$$\Delta P = \frac{g P_{atm}}{R} \left( \frac{1}{T_b} - \frac{1}{T_f} \right) z \quad (4)$$

where

- $T_b$  = absolute temperature outside the fire space,
- $T_f$  = absolute temperature of gas in the fire compartment,
- $P_{atm}$  = absolute atmospheric pressure,
- $R$  = gas constant of air,
- $g$  = acceleration of gravity, and
- $z$  = height above the neutral plane.

For runs 8 and 9, the neutral plane between the fire compartment and its surroundings is estimated at about 1.3 m (4.2 ft) above the floor. The opening between floor one and the shaft extends from the floor to 2 m (6.6 ft) above the floor. Both the pressure difference due to fire gas buoyancy and the pressure difference due to stack effect are evaluated at the top of this opening. Thus the height above the neutral plane,  $z$ , is 0.7 m (2.3 ft). The other parameters are  $T_b = 294$  K (530°R),  $T_f = 773$  K (1390°R),  $P_{atm} = 101325$  Pa (407.3 in H<sub>2</sub>O),  $R = 287$  (1716),  $g = 9.8$  m/s<sup>2</sup> (32.2 ft/s<sup>2</sup>). From equation (4), the pressure difference due to buoyancy of fire gases is 5 Pa (0.02 in H<sub>2</sub>O).

The pressure difference due to reverse stack effect is calculated from equation (1) at 11 Pa (0.04 in H<sub>2</sub>O) using the following parameters:  $T_o = 310$  K (558°R),  $T_s = 294$  K (530°R),  $z = -18$  m (-59 ft). Explanations are in order concerning the distance,  $z$ , from the neutral plane and the meaning of  $\Delta P$  from equation (1). In this case the neutral plane in question is that between the shaft and the outside. The location of this neutral plane is taken to be approximately at the mid height of the building. Then the distance from the neutral plane to the top of the opening between the first floor and the shaft is -18 m (-59 ft).

The pressure difference,  $\Delta P$ , from equation (1) is from the shaft to the outside. This pressure difference is the sum of the pressure difference,  $\Delta P_{sf}$ , from the shaft to the floor and the pressure difference,  $\Delta P_{fo}$ , from the floor to the outside ( $\Delta P = \Delta P_{sf} + \Delta P_{fo}$ ). In general the concept of effective flow areas (Klote and Milke 1992) needs to be used to evaluate  $\Delta P_{sf}$  and  $\Delta P_{fo}$ . However, this problem is simplified because the first floor opening to the outside is 100 times that from the shaft to the building. In this case, the pressure of the fire floor is almost the same as that outside, and so  $\Delta P_{fo}$  can be neglected. Thus  $\Delta P$  is nearly equal to  $\Delta P_{sf}$  when the opening to the outside is very large compared to the opening between the shaft and the floor. Therefore, the results of equation (1) can be used without modification in this case.

Because the pressure difference due to reverse stack effect [11 Pa (0.04 in H<sub>2</sub>O)] is greater than that due to fire gas buoyancy [5 Pa (0.02 in H<sub>2</sub>O)], it is estimated that smoke will not flow into the shaft. This agrees with the computer simulations.

## 6.4 3rd Floor Fire and Reverse Stack Effect

Runs 10, 11 and 12 have a 2 MW fire on the third floor with the summer outside temperature. These runs were made to see the impact of reverse stack effect at floor 3 on smoke flow. Runs 10 and 11 both used the two zone shaft model, which is inappropriate for the reasons already discussed. For runs 10 and 11, this shaft model develops an upper layer in the shaft (figures 20, 22 and 24) which results in formation of an upper layer on floor 8 (figures 19, 21 and 23) at about 25 minutes after fire ignition. These figure also show that the one zone shaft model results in no upper layer on floor 8 and in low levels of temperature and CO in the shaft (about 26°C (79°F) and 0.05% CO). As with the other simulation, HVAC heating did not make a significant difference.

## 6.5 Layer Initiation Temperature

For all of the runs above, the layer initiation temperature difference was 40°C (72°F). Runs 16, 17 and 18 were conducted with a layer initiation temperature difference of 1°C (1.8°F) to see how this impacts the simulations. Run 16 is the same as run 6, except for the initiation temperature. These runs do not



include a fire. For run 6 with the high initiation temperature, no upper layers were formed. However, for run 16 with the low initiation temperature, upper layers were formed as shown in figure 31. Figure 32 is a comparison of temperatures for these runs. The upper layer temperatures from run 16 are higher than their corresponding lower layer temperatures from run 6. The temperature differences are all less than 15°C (27°F). Differences of this magnitude could have some significance when evaluating tenability.

Run 17 is the same as run 12 except for initiation temperature. Run 12 was of a 2 MW fire on the third floor during reverse stack effect. Both runs use the one zone shaft model, and by definition there is no upper level in the shaft (figure 34). The temperatures and CO concentrations in the shaft are for both simulations (figures 36 and 37). In run 12 no upper layer was formed on floor 8, but one forms there in run 17. The interface for this layer descended to about 0.5 m (1.6 ft) (figure 33). However, this upper layer temperature is no more than 6°C (11°F) above the lower layer temperature of run 12 (figure 35).

Run 18 is the same as run 15 except for initiation temperature. Run 15 was the 2 MW fire on the first floor during normal stack effect with large openings between the shaft and the building. Examination of figures 38, 39 and 41 shows that with the lower initiation temperature (run 18), there is no delay in forming the upper layer on floor 8. These same figures show that with a large initiation temperature (run 15), there is a delay on the order of 2 minutes. After this delay, the temperature and CO level on floor 8 from run 15 approach those from run 18. After about 20 minutes, the temperature and CO level on floor 8 are almost the same for these two runs. Thus, the initiation temperature does not seem to make a significant impact on fire conditions in the long run. However, in the short run, the differences might be important, especially concerning tenability.

## 7. Future Effort

NIST's Large Scale Smoke Movement Project includes experimental study of smoke movement in both open shafts and stair shafts. Computational fluid dynamics will be used as an aid to this experimental study. Based on understanding of relevant mechanisms gained from this study, first order models will be developed for open shafts and stair shafts. These models will be appropriate for incorporation into zone fire models.

## 8. Conclusions

1. The smoke flow of two zone shaft models is inconsistent with smoke flow in tall shafts. For this paper, tall shafts are ones with aspect ratios much greater than 2. Further research is needed to understand the relevant mechanisms so that a shaft smoke flow model can be developed which can be integrated into two zone models and simulate smoke flow under the wide range of driving forces that occur in buildings.
2. The two zone shaft model is applicable for short shafts. For this paper, short shafts are ones with aspect ratios less than two. The probability of plume contact with the walls of short shafts is low.
3. The zero order (one zone) shaft model used in this paper can not be expected to realistically simulate smoke flow in many situations. For example when the natural forces produce a shaft counter flow or when smoke mixing occurs for only a fraction of the shaft volume. However, the

simulations using the zero order model seem less unrealistic than those using the two zone simulations.

4. Further research is needed to develop first order models of smoke flow in open shafts and stair shafts for tall shafts subject to natural building flows.
5. The selection of the upper layer initiation temperature does not make a significant difference with respect to gross smoke movement due to large fires. However, selection of the initiation temperature may have significant consequences concerning tenability calculations.
6. HVAC heating is not significant with respect to gross smoke movement due to large fires. However, this feature could be added to other zone fire models. HVAC heating would be useful in validating the stack effect treatment of other zone fire models, and it may be useful for some tenability calculations.

## 9. References

- Best, R. and Demers, D.P. 1982. Investigation Report on the MGM Grand Hotel Fire - Las Vegas, Nevada, November 21, 1980, National Fire Protection Association, Quincy, MA.
- Bukowski, R.W., Peacock, R.D., Jones, W.W. and Forney, C.L. 1991. Technical Reference Guide for HAZARD I Fire Hazard Assessment Method, Version 1.1, NIST Handbook 146, Vol II, National Institute of Standards and Technology, Gaithersburg, MD.
- Bukowski, R.W. 1991. Fire Models, the Future is Now!, NFPA Journal, No 85, Vol 2, pp 60-69, March/April.
- Cannon, J.B. and Zukoski, E.E. 1976. Turbulent Mixing in Vertical Shafts Under Conditions Applicable to Fires in High Rise Buildings, California Institute of Technology, Pasadena, CA.
- Cooper, L.Y. and Forney, G.P. 1990. The Consolidated Compartment Fire Model (CCFM) Computer Code Application CCFM.VENTS - Part I: Physical Basis.
- Cooper, L.Y. 1985. ASET - A Computer Program for Calculating Available Safe Egress Time, Fire Safety Journal, Vol 9, pp 29-45.
- Davis, W.D. and Cooper, L.Y. 1989. Estimating the Environment and the Sprinkler Links in Compartment Fires With Draft Curtains and Fusible-Link-Actuated Ceiling Vents - Part II: User Guide for the Computer Code LAVENT, National Institute of Standards and Technology, NISTIR 89-4122.
- Evers, E. and Waterhouse, A. 1978. A Computer Model for Analyzing Smoke Movement in Buildings, Building Research Est., Borehamwood, Herts, U.K.
- Jones, W.W. 1983. A Review of Compartment Fire Models, Nat. Bur. of Stand. (U.S.), NBSIR 83-2684.

- Juillerant, E.E. 1964. Jacksonville Hotel Disaster, NFPA Quarterly, Vol 57, No 4, pp 309-319.
- Klote, J.H. 1991. A General Routine for Analysis of Stack Effect, National Institute of Standards and Technology, NISTIR 4588.
- Klote, J.H. 1990. Fire Experiments of Zoned Smoke Control at the Plaza Hotel in Washington DC, ASHRAE Transactions, Vol. 96, Part 2, pp 399-416.
- Klote, J.H. and Milke, J.A. 1992. Design of Smoke Management Systems, American Society of Heating, Refrigerating and Air-Conditioning Engineers, Atlanta, GA.
- Marshall, N.R. 1986. Air entrainment into smoke and hot gases in open shafts, Fire Safety Journal, Vol 10, No 1, pp 37-46.
- Marshall, N.R. 1985. The behaviour of hot gases flowing within a staircase, Fire Safety Journal, Vol 9, No 3, pp 245-255.
- McGuire, J.H. and Tamura G.T 1975. Simple Analysis of Smoke-Flow Problems in High Buildings, Fire Technology, Vol 11, No 1, pp 15-22.
- Mitler, H.E. and Emmons, H.W. 1981. Documentation for CFC V, the fifth Harvard computer code. Home Fire Project Tech. Rep. #45, Harvard University.
- Mitler, H.E. and Rockett, J.A. 1986. How Accurate is Mathematical Fire Modeling?, Nat. Bur. Stand. (U. S.), NBSIR 86-3459.
- Mitler, H.E. 1985. Comparison of Several Compartment Fire Models: An Interim Report, Nat. Bur. of Stand. (U.S.), NBSIR 85-3233.
- Peacock, R.D., Jones, W.W., Bukowski, R.W., and Forney, C.L. 1991. Software User's Guide for HAZARD I, Version 1.1, NIST Handbook 146, Vol I, National Institute of Standards and Technology, Gaithersburg, MD.
- Peacock, R.D., Forney, G.P., Reneke, P., Portier, R. and Jones, W.W. 1993. CFAST, the Consolidated Model of Fire Growth and Smoke Transport, National Institute of Standards and Technology, NIST Technical Note 1299.
- Quintiere, J.G. 1989. Fundamentals of Enclosure Fire "Zone" Models, Journal of Fire Protection Engineering, Vol 1, No 3, pp 99-119.
- Said, M.N.A. 1988. A Review of Smoke Control Models, ASHRAE Journal, Vol 30, No 4, pp 36-40.
- Steckler, K., Quintiere, J.G. and Klote, J.H. 1990. The Johnson City Fire, (Letter Report), Center for Fire Research, National Institute of Standards and Technology, Gaithersburg, MD.
- Tanaka, T. 1983. A Model of Multiroom Fire Spread. Nat. Bur. of Stand. (U.S.), NBSIR 83-2718.



NIST-114 (REV. 9-92) ADMAN 4.09	<b>U.S. DEPARTMENT OF COMMERCE</b> <b>NATIONAL INSTITUTE OF STANDARDS AND TECHNOLOGY</b>	<b>(ERB USE ONLY)</b>																
<b>MANUSCRIPT REVIEW AND APPROVAL</b>		ERB CONTROL NUMBER .....	DIVISION .....															
		PUBLICATION REPORT NUMBER NISTIR 5251	CATEGORY CODE .....															
INSTRUCTIONS: ATTACH ORIGINAL OF THIS FORM TO ONE (1) COPY OF MANUSCRIPT AND SEND TO: THE SECRETARY, APPROPRIATE EDITORIAL REVIEW BOARD.		PUBLICATION DATE September 1993	NUMBER PRINTED PAGES .....															
TITLE AND SUBTITLE (CITE IN FULL)  Zone Fire Modeling with Natural Building Flows and a Zero Order Shaft Model																		
CONTRACT OR GRANT NUMBER .....		TYPE OF REPORT AND/OR PERIOD COVERED .....																
AUTHOR(S) (LAST NAME, FIRST INITIAL, SECOND INITIAL)  Klote, John H. and Forney, Glenn P.		PERFORMING ORGANIZATION (CHECK (X) ONE BOX) <input checked="" type="checkbox"/> NIST/GAITHERSBURG <input type="checkbox"/> NIST/BOULDER <input type="checkbox"/> JILA/BOULDER																
LABORATORY AND DIVISION NAMES (FIRST NIST AUTHOR ONLY) Building and Fire Research Laboratory, Fire Safety Engineering Division																		
SPONSORING ORGANIZATION NAME AND COMPLETE ADDRESS (STREET, CITY, STATE, ZIP) .....																		
RECOMMENDED FOR NIST PUBLICATION <table style="width: 100%;"> <tr> <td><input type="checkbox"/> JOURNAL OF RESEARCH (NIST JRES)</td> <td><input type="checkbox"/> MONOGRAPH (NIST MN)</td> <td><input type="checkbox"/> LETTER CIRCULAR</td> </tr> <tr> <td><input type="checkbox"/> J. PHYS. &amp; CHEM. REF. DATA (JPCRD)</td> <td><input type="checkbox"/> NATL. STD. REF. DATA SERIES (NIST NSRDS)</td> <td><input type="checkbox"/> BUILDING SCIENCE SERIES</td> </tr> <tr> <td><input type="checkbox"/> HANDBOOK (NIST HB)</td> <td><input type="checkbox"/> FEDERAL INF. PROCESS. STDS. (NIST FIPS)</td> <td><input type="checkbox"/> PRODUCT STANDARDS</td> </tr> <tr> <td><input type="checkbox"/> SPECIAL PUBLICATION (NIST SP)</td> <td><input type="checkbox"/> LIST OF PUBLICATIONS (NIST LP)</td> <td><input type="checkbox"/> OTHER _____</td> </tr> <tr> <td><input type="checkbox"/> TECHNICAL NOTE (NIST TN)</td> <td><input checked="" type="checkbox"/> NIST INTERAGENCY/INTERNAL REPORT (NISTIR)</td> <td></td> </tr> </table>				<input type="checkbox"/> JOURNAL OF RESEARCH (NIST JRES)	<input type="checkbox"/> MONOGRAPH (NIST MN)	<input type="checkbox"/> LETTER CIRCULAR	<input type="checkbox"/> J. PHYS. & CHEM. REF. DATA (JPCRD)	<input type="checkbox"/> NATL. STD. REF. DATA SERIES (NIST NSRDS)	<input type="checkbox"/> BUILDING SCIENCE SERIES	<input type="checkbox"/> HANDBOOK (NIST HB)	<input type="checkbox"/> FEDERAL INF. PROCESS. STDS. (NIST FIPS)	<input type="checkbox"/> PRODUCT STANDARDS	<input type="checkbox"/> SPECIAL PUBLICATION (NIST SP)	<input type="checkbox"/> LIST OF PUBLICATIONS (NIST LP)	<input type="checkbox"/> OTHER _____	<input type="checkbox"/> TECHNICAL NOTE (NIST TN)	<input checked="" type="checkbox"/> NIST INTERAGENCY/INTERNAL REPORT (NISTIR)	
<input type="checkbox"/> JOURNAL OF RESEARCH (NIST JRES)	<input type="checkbox"/> MONOGRAPH (NIST MN)	<input type="checkbox"/> LETTER CIRCULAR																
<input type="checkbox"/> J. PHYS. & CHEM. REF. DATA (JPCRD)	<input type="checkbox"/> NATL. STD. REF. DATA SERIES (NIST NSRDS)	<input type="checkbox"/> BUILDING SCIENCE SERIES																
<input type="checkbox"/> HANDBOOK (NIST HB)	<input type="checkbox"/> FEDERAL INF. PROCESS. STDS. (NIST FIPS)	<input type="checkbox"/> PRODUCT STANDARDS																
<input type="checkbox"/> SPECIAL PUBLICATION (NIST SP)	<input type="checkbox"/> LIST OF PUBLICATIONS (NIST LP)	<input type="checkbox"/> OTHER _____																
<input type="checkbox"/> TECHNICAL NOTE (NIST TN)	<input checked="" type="checkbox"/> NIST INTERAGENCY/INTERNAL REPORT (NISTIR)																	
RECOMMENDED FOR NON-NIST PUBLICATION (CITE FULLY)		PUBLISHING MEDIUM <input type="checkbox"/> PAPER <input type="checkbox"/> CD-ROM <input type="checkbox"/> DISKETTE (SPECIFY) _____ <input type="checkbox"/> OTHER (SPECIFY) _____																
SUPPLEMENTARY NOTES .....																		
ABSTRACT (A 1500-CHARACTER OR LESS FACTUAL SUMMARY OF MOST SIGNIFICANT INFORMATION. IF DOCUMENT INCLUDES A SIGNIFICANT BIBLIOGRAPHY OR LITERATURE SURVEY, CITE IT HERE. SPELL OUT ACRONYMS ON FIRST REFERENCE.) (CONTINUE ON SEPARATE PAGE, IF NECESSARY.)  This paper addresses applications of zone fire models to simulate smoke flow in multistory buildings. Natural flows in buildings are discussed. A zero order model for shaft smoke flow was developed which treated the shaft as one perfectly mixed zone. A two zone fire model was modified to simulate natural flows and the zero order shaft smoke flow. The extent to which the one zone model and the two zone model are appropriate to simulate smoke flow in shafts is discussed. The modifications for the natural building flow included development of new initial conditions and of the capability to simulate the gross effects of a heating and air conditioning system. Eighteen example zone model simulations were made to develop insight into the program modifications.																		
KEY WORDS (MAXIMUM 9 KEY WORDS; 28 CHARACTERS AND SPACES EACH; ALPHABETICAL ORDER; CAPITALIZE ONLY PROPER NAMES)  air movement; fire models; smoke movement; stairwells; zone models																		
AVAILABILITY <input checked="" type="checkbox"/> UNLIMITED <input type="checkbox"/> FOR OFFICIAL DISTRIBUTION. DO NOT RELEASE TO NTIS. <input type="checkbox"/> ORDER FROM SUPERINTENDENT OF DOCUMENTS, U.S. GPO, WASHINGTON, D.C. 20402 <input checked="" type="checkbox"/> ORDER FROM NTIS, SPRINGFIELD, VA 22161		NOTE TO AUTHOR(S) IF YOU DO NOT WISH THIS MANUSCRIPT ANNOUNCED BEFORE PUBLICATION, PLEASE CHECK HERE. <input type="checkbox"/>																

ELECTRONIC FORM







